Review

Mechanisms of oxidation by *trans*-dioxoruthenium(VI) complexes containing macrocyclic tertiary amine ligands

William W.Y. Lam, Wai-Lun Man, Tai-Chu Lau *

Department of Biology and Chemistry, City University of Hong Kong, Tat Chee Avenue, Kowloon Tong, Hong Kong, China

Contents

Abstract

This review summarizes the kinetics and mechanisms of the oxidation of various inorganic and organic substrates by *trans*-dioxoruthenium(VI) complexes containing macrocyclic tertiary amine ligands during the period 1993–2006.
© 2007 Elsevier B.V. All rights reserved.

Keywords: Ruthenium; Oxo; Kinetics; Macrocyclic ligands; Oxidation

1. Introduction

The chemistry of ruthenium oxo complexes has received much attention during the past 20 years. In particular Meyer and co-workers [1] and others have shown that ruthenium(IV) oxo complexes containing polypyridyl ligands such as [(bpy)$_2$(py)Ru^{IV}O]$^{2+}$ are powerful oxidants that can oxidize substrates by a variety of mechanisms, including electron transfer [1b], proton-coupled electron transfer [1c–e], hydrogen atom abstraction [1f–i,2], hydride abstraction [1j–m], and oxygen atom transfer [1n,s].
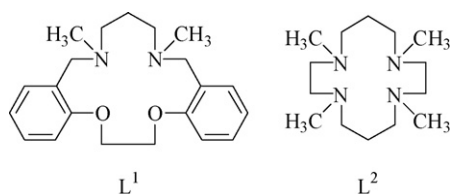
Fig. 1. Structure of L^1 and L^2.

Another class of ruthenium oxo complexes that are potent oxidants are *trans*-dioxoruthenium(VI) complexes, *trans*-$[Ru^{VI}(L)(O)_2]^{2+}$, especially those containing macrocyclic tertiary amine ligands, which were reported by Che et al. [3]. The coordinated macrocyclic ligand L (L = L^1, L^2; Fig. 1) is resistant to oxidative degradation and ligand exchange. The lower oxidation states of these complexes (V–II) are also well-characterized, thus facilitating identification of products and mechanistic interpretations. These complexes are milder oxidants than $[(bpy)_2(py)Ru^{IV}O]^{2+}$, so substrates that are too rapidly oxidized by $[(bpy)_2(py)Ru^{IV}O]^{2+}$ may be studied with these

complexes. Because of the difference in redox potentials and electron-transfer properties, oxidation of substrates by *trans*-$[Ru^{VI}(L)(O)_2]^{2+}$ often occurs by mechanisms different from that by $[(bpy)_2(py)Ru^{IV}O]^{2+}$. The present review is confined to the kinetics and mechanisms of the oxidation of various inorganic and organic substrates by *trans*-$[Ru^{VI}(L)(O)_2]^{2+}$ mainly during the period 1993–2006. The kinetics of the oxidation of substitution inert ruthenium(II) complexes and the disproportionation of *trans*-$[Ru^{V}(L^2)(O)_2]^+$ [4], which were reported in 1990, were also discussed in order to give a more complete picture of the reactivity of these dioxoruthenium(VI) species. The chemistry of ruthenium oxo species before this period has been reviewed [5].

2. Electrochemical and electron-transfer properties

The electrochemical properties of *trans*-$[Ru^{VI}(L)(O)_2]^{2+}$ have been reviewed. Thermodynamic data (E° versus NHE and pK_a values, 298 K) for *trans*-$[Ru^{VI}(L)(O)_2]^{2+}$ systems in aqueous solutions are summarized in Scheme 1 [5–7].
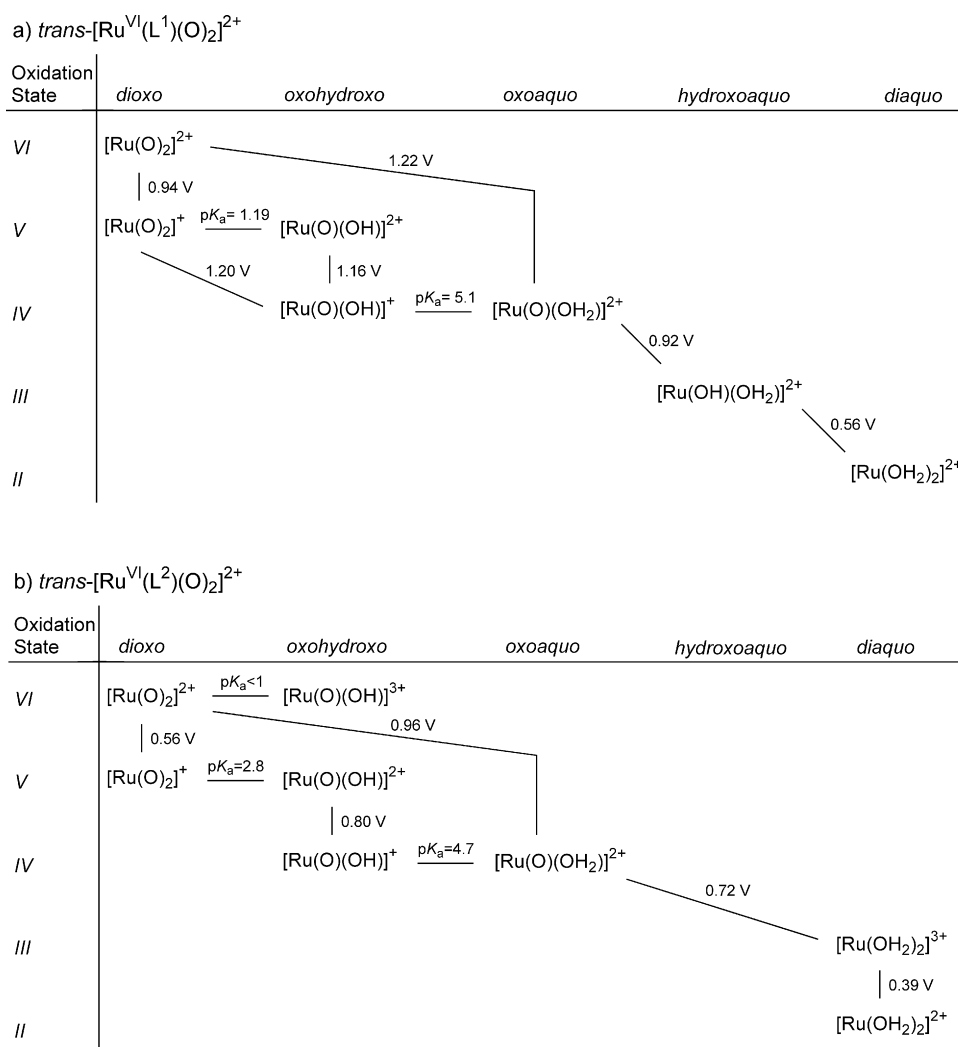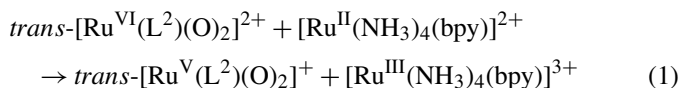

Scheme 1.

3. Reaction with inorganic substrates

3.1. Oxidation of substitution inert ruthenium(II) complexes [4]

Reaction of excess *trans*-$[Ru^{VI}(L^2)(O)_2]^{2+}$ with $[Ru^{II}(NH_3)_4$ (bpy)$]^{2+}$ in aqueous solution occurs according to the following stoichiometry:

trans-$[Ru^{VI}(L^2)(O)_2]^{2+} + [Ru^{II}(NH_3)_4(bpy)]^{2+}$

$$\rightarrow \textit{trans-}[Ru^V(L^2)(O)_2]^+ + [Ru^{III}(NH_3)_4(bpy)]^{3+} \quad (1)$$

The *trans*-$[Ru^V(L^2)(O)_2]^+$ species then undergoes rapid disproportionation (see Section 3.2). Reaction (1) has the following rate law:

$$-\frac{d[Ru^{II}]}{dt} = k_2[Ru^{VI}][Ru^{II}] \quad (2)$$

k_2 is independent of pH from 1.0 to 4.0. At 298.0 K, k_2 is $(2.4 \pm 0.1) \times 10^6 \, M^{-1} \, s^{-1}$ at $I = 0.1 \, M$ and $(6.1 \pm 0.3) \times 10^5 \, M^{-1} \, s^{-1}$ at $I = 0.01 \, M$. $\Delta H^{\ddagger}$ and $\Delta S^{\ddagger}$ are (1.1 ± 0.1) kcal mol^{-1} and $-(28 \pm 5)$ cal mol^{-1} K^{-1}, respectively, at $I = 0.01 \, M$. The kinetics of the oxidation of $[Ru^{II}(NH_3)_5(isn)]^{2+}$ and $[Ru^{II}(NH_3)_5(py)]^{2+}$ have also been studied, the second-order rate constants at 298.0 K are $(3.0 \pm 0.1) \times 10^6$ ($I = 0.1 \, M$) and $(3.4 \pm 0.1) \times 10^6 \, M^{-1} \, s^{-1}$ ($I = 0.01 \, M$), respectively. Using the Marcus cross-relation [8], the self-exchange rate of the *trans*-$[Ru^{VI}(L^2)(O)_2]^{2+/+}$ couple is estimated to be $1.5 \times 10^5 \, M^{-1} \, s^{-1}$ (298.0 K and $I = 0.1 \, M$).

3.2. Disproportionation of trans-$[Ru^V(L^2)(O)_2]^+$ [4]

In aqueous acidic solutions the cyclic voltammogram of *trans*-$[Ru^{VI}(L^2)(O)_2]^{2+}$ shows a two-proton two-electron Ru^{VI}/Ru^{IV} couple, suggesting that the intermediate Ru^V state is unstable with respect to disproportionation. The kinetics of the disproportionation reaction have been studied by generating Ru^V *in situ* by reduction of *trans*-$[Ru^{VI}(L^2)(O)_2]^{2+}$ with $[Ru^{II}(NH_3)_4(bpy)]^{2+}$. The following rate law is obtained:

$$-\frac{d[Ru^V]}{dt} = k_{dis}[Ru^V]^2 \quad (3)$$

$$k_{dis} = \frac{2k_e K_p[H^+]}{(1 + K_p[H^+])^2} \quad (4)$$

This is consistent with the following mechanism:

trans-$[Ru^V(L^2)(O)_2]^+ + H^+ \overset{K_p}{\rightleftharpoons} \textit{trans-}[Ru^V(L^2)(O)(OH)]^{2+}$

$$(5)$$

trans-$[Ru^V(L^2)(O)(OH)]^{2+} + \textit{trans-}[Ru^V(L^2)(O_2)]^+$

$$\overset{k_e}{\longrightarrow} \textit{trans-}[Ru^{VI}(L^2)(O)_2]^{2+} + \textit{trans-}[Ru^{IV}(L^2)(O)(OH)]^+$$

$$(6)$$

trans-$[Ru^{IV}(L^2)(O)(OH)]^+ + H^+$

$$\overset{fast}{\longrightarrow} \textit{trans-}[Ru^{IV}(L^2)(O)(OH_2)]^{2+} \quad (7)$$
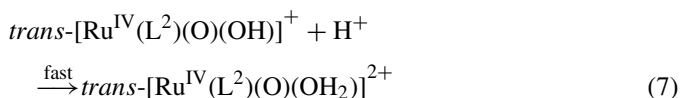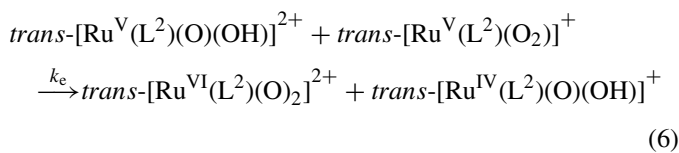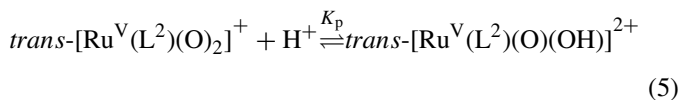
k_e and K_p are found to be $(2.72 \pm 0.34) \times 10^6 \, M^{-1} \, s^{-1}$ and $(615 \pm 50) \, M^{-1}$, respectively, at 299 K and $I = 0.1 \, M$. $\Delta H^{\ddagger}$ and $\Delta S^{\ddagger}$ for the k_e step are (4.5 ± 0.7) kcal mol^{-1} and $-(14 \pm 2)$ cal mol^{-1} K^{-1}, respectively.

3.3. Oxidation of $[Fe^{II}(OH_2)_6]^{2+}$ [9]

In aqueous acidic solution, oxidation of excess $[Fe^{II}(OH_2)_6]^{2+}$ by *trans*-$[Ru^{VI}(L^2)(O)_2]^{2+}$ readily occurs at room temperature according to the following equation:

trans-$[Ru^{VI}(L^2)(O)_2]^{2+} + 2Fe^{2+} + 2H^+$

$$\rightarrow \textit{trans-}[Ru^{IV}(L^2)(O)(OH_2)]^{2+} + 2Fe^{3+} \quad (8)$$
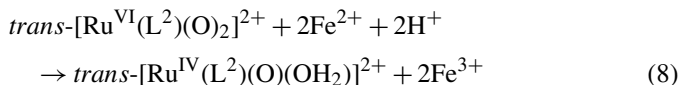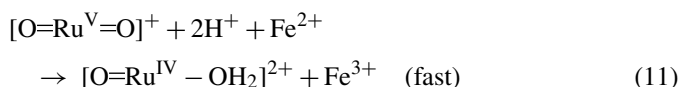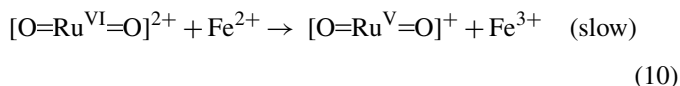
The kinetics are followed by UV/vis spectrophotometry. The rate law is:

$$-\frac{d[Ru^{VI}]}{dt} = k_2[Ru^{VI}][Fe^{2+}] \quad (9)$$

At 298 K and $I = 1.0 \, M$, k_2 is found to be $(2.74 \pm 0.08) \times 10 \, M^{-1} \, s^{-1}$. k_2 is independent of $[H^+]$ from 0.01 to 1.0 M and is rather insensitive to temperature from 291 to 311 K. At $[H^+]$ and $I = 0.1 \, M$, $\Delta H^{\ddagger}$ and $\Delta S^{\ddagger}$ are (0.1 ± 0.1) kcal mol^{-1} and $-(50 \pm 5)$ cal mol^{-1} K^{-1}, respectively.

The proposed mechanism that is consistent with the simple rate law is shown below.

$$[O=Ru^{VI}=O]^{2+} + Fe^{2+} \rightarrow [O=Ru^V=O]^+ + Fe^{3+} \quad (slow)$$

$$(10)$$

$$[O=Ru^V=O]^+ + 2H^+ + Fe^{2+}$$

$$\rightarrow [O=Ru^{IV}-OH_2]^{2+} + Fe^{3+} \quad (fast) \quad (11)$$

Using a self-exchange rate of $4 \, M^{-1} \, s^{-1}$ for Fe^{2+}/Fe^{3+} [10], the value of k_{12} is estimated to be $10 \, M^{-1} \, s^{-1}$. This calculated value compares favorably with the measured value of $27 \, M^{-1} \, s^{-1}$ at $I = 1.0 \, M$. However, it has been suggested that a more realistic value for the $Fe(OH_2)_6^{2+/3+}$ is $6 \times 10^{-3} \, M^{-1} \, s^{-1}$, since the $Fe(OH_2)_6^{2+/3+}$ is probably inner-sphere with a bridging water molecule [11–13]. Using this value, k_{12} is calculated to be $0.5 \, M^{-1} \, s^{-1}$. Moreover, the observed zero $\Delta H^{\ddagger}$ is consistent with an inner-sphere mechanism (Eqs. (12) and (13)) in which the formation of the bridged intermediate is exothermic and hence offsets the activation enthalpy for electron transfer.

$$[O=Ru^{VI}=O]^{2+} + Fe^{2+} \rightleftharpoons [O=Ru^{VI}=O-Fe]^{4+} \quad (12)$$

$$[O=Ru^{VI}=O-Fe]^{4+} \rightarrow [O=Ru^V=O]^+ + Fe^{3+} \quad (13)$$
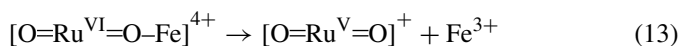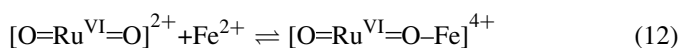
3.4. Oxidation of sulfite [14]

The kinetics of the oxidation of SO_3^{2-} by *trans*-$[Ru^{VI}(L^2)(O)_2]^{2+}$ have been studied in aqueous solution at

298.0 K. The reaction has the following stoichiometry:

$$\textit{trans-}[Ru^{VI}(L^2)(O)_2]^{2+} + SO_3^{2-} + H_2O$$
$$\rightarrow \textit{trans-}[Ru^{IV}(L^2)(O)(OH_2)]^{2+} + SO_4^{2-} \qquad (14)$$
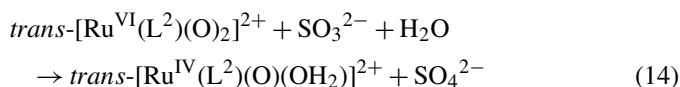
The rate law is:

$$-\frac{d[Ru^{VI}]}{dt} = \frac{k}{1 + [H^+]/K_a}[Ru^{VI}][S^{IV}] \qquad (15)$$

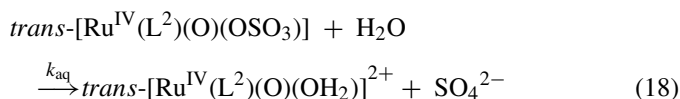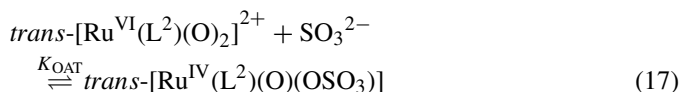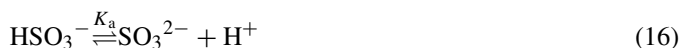At 298.0 K and $I = 1.0$ M, k and K_a are found to be $(7.0 \pm 1.4) \times 10^4$ M^{-1} s^{-1} and $(3.4 \pm 1.0) \times 10^{-7}$ M, respectively.

The theoretical value for outer-sphere electron transfer between SO_3^{2-} and $\textit{trans-}[Ru^{VI}(L^2)(O)_2]^{2+}$ is calculated to be 6.3×10^2 M^{-1} s^{-1} at 298 K by using the Marcus cross-relation, which is smaller than k by over two orders of magnitude, suggesting that an inner-sphere type of mechanism is operating. Oxidation of sulfite by one-electron oxidants is usually affected by air, due to the formation of the $SO_3^{\bullet-}$ intermediate [15]. In this case the kinetics are unaffected by the presence of O_2, suggesting that a one-electron mechanism is less unlikely. An OAT mechanism is proposed:

$$HSO_3^- \overset{K_a}{\rightleftharpoons} SO_3^{2-} + H^+ \qquad (16)$$

$$\textit{trans-}[Ru^{VI}(L^2)(O)_2]^{2+} + SO_3^{2-}$$
$$\overset{K_{OAT}}{\rightleftharpoons} \textit{trans-}[Ru^{IV}(L^2)(O)(OSO_3)] \qquad (17)$$

$$\textit{trans-}[Ru^{IV}(L^2)(O)(OSO_3)] + H_2O$$
$$\overset{k_{aq}}{\longrightarrow} \textit{trans-}[Ru^{IV}(L^2)(O)(OH_2)]^{2+} + SO_4^{2-} \qquad (18)$$

The measured value of K_a (3.4×10^{-7} M) is in reasonable agreement with a literature value (1.2×10^{-7} M) [16].

3.5. Oxidation of iodide [17]

The kinetics of the oxidation of iodide by $\textit{trans-}[Ru^{VI}(L^2)(O)_2]^{2+}$ have been studied in aqueous acidic solution. The reaction has the following stoichiometry:

$$\textit{trans-}[Ru^{VI}(L^2)(O)_2]^{2+} + 3I^- + 2H^+$$
$$\rightarrow \textit{trans-}[Ru^{IV}(L^2)(O)(OH_2)]^{2+} + I_3^- \qquad (19)$$
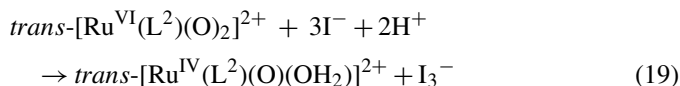
The rate law is:

$$-\frac{d[Ru^{VI}]}{dt} = (k_a + k_b[H^+])[Ru^{VI}][I^-] \qquad (20)$$

At 298.0 K and $I = 0.1$ M, k_a and k_b are found to be $(4.1 \pm 1.3) \times 10^{-2}$ M^{-1} s^{-1} and (18.5 ± 0.2) M^{-2} s^{-1}, respectively. The effects of temperature on k_a and k_b, have been studied from 290.0 to 318.0 K. For the k_a path, $\Delta H^{\ddagger}$ and $\Delta S^{\ddagger}$ are (10.3 ± 2.2) kcal mol^{-1} and $-(31 \pm 10)$ cal mol^{-1} K^{-1}, respectively; while for the k_b path, $\Delta H^{\ddagger}$ and $\Delta S^{\ddagger}$ are (8.8 ± 0.7) kcal mol^{-1} and $-(23 \pm 2)$ cal mol^{-1} K^{-1}.

The one-electron outer-sphere oxidation of iodide has been studied for many complexes under conditions where the reverse reaction is negligible [18]. The stoichiometry and rate law are shown in Eqs. (21) and (22), respectively.
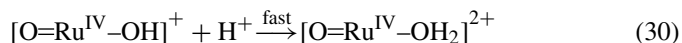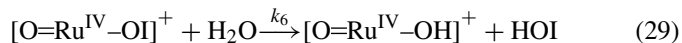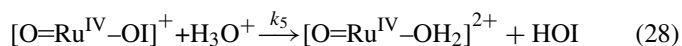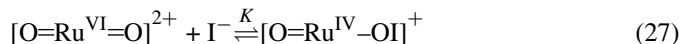
$$2M_{OX} + 2I^- \rightarrow 2M_{red} + I_2 \qquad (21)$$

$$-\frac{d[M_{OX}]}{dt} = 2k_1[M_{OX}][I^-] + 2k_2[M_{OX}][I^-]^2 \qquad (22)$$

The general mechanism is shown in Eqs. (23)–(26).

$$M_{OX} + I^- \underset{k_{-1}}{\overset{k_1}{\rightleftharpoons}} M_{red} + I^\bullet \qquad (23)$$

$$M_{OX} + 2I^- \underset{k_{-2}}{\overset{k_2}{\rightleftharpoons}} M_{red} + I_2^{\bullet-} \qquad (24)$$

$$M_{OX} + I_2^{\bullet-} \underset{k_{-3}}{\overset{k_3}{\rightleftharpoons}} M_{red} + I_2 \qquad (25)$$

$$I^\bullet + I^- \underset{k_{-4}}{\overset{k_4}{\rightleftharpoons}} I^{\bullet-} \qquad (26)$$

In the oxidation by $\textit{trans-}[Ru^{VI}(L^2)(O)_2]^{2+}$ the observed first order dependence of the rate on $[I^-]$ is not consistent with a simple one-electron outer-sphere mechanism, and an OAT mechanism is proposed. The proposed mechanism (Eqs. (27)–(31)) involves rapid oxygen atom transfer from Ru(VI) to iodide followed by rate-limiting acid-catalyzed aquation of the resulting Ru^{IV}–OI species.

$$[O=Ru^{VI}=O]^{2+} + I^- \overset{K}{\rightleftharpoons} [O=Ru^{IV}-OI]^+ \qquad (27)$$

$$[O=Ru^{IV}-OI]^+ + H_3O^+ \overset{k_5}{\longrightarrow} [O=Ru^{IV}-OH_2]^{2+} + HOI \qquad (28)$$

$$[O=Ru^{IV}-OI]^+ + H_2O \overset{k_6}{\longrightarrow} [O=Ru^{IV}-OH]^+ + HOI \qquad (29)$$

$$[O=Ru^{IV}-OH]^+ + H^+ \overset{fast}{\longrightarrow} [O=Ru^{IV}-OH_2]^{2+} \qquad (30)$$

$$HOI + I^- + H^+ \overset{fast}{\longrightarrow} I_2 + H_2O \qquad (31)$$
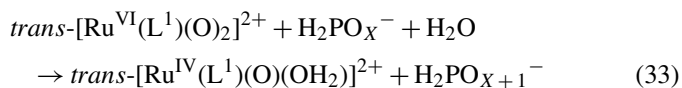
According to this mechanism the rate law is:

$$\text{Rate} = K(k_6 + k_5[H^+])[Ru^{VI}][I^-] \qquad (32)$$

This agrees with the experimental rate law with $k_a = Kk_6$ and $k_b = Kk_5$.

3.6. Oxidation of hypophosphite and phosphite [19]

The kinetics of the oxidation of hypophosphite and phosphite by $\textit{trans-}[Ru^{VI}(L^1)(O)_2]^{2+}$ have been studied in aqueous acidic solutions. The reactions have the following stoichiometry ($X = 2$ or 3):

$$\textit{trans-}[Ru^{VI}(L^1)(O)_2]^{2+} + H_2PO_X^- + H_2O$$
$$\rightarrow \textit{trans-}[Ru^{IV}(L^1)(O)(OH_2)]^{2+} + H_2PO_{X+1}^- \qquad (33)$$

The two reactions also have the same rate law ($P = P^I$ or P^{III}):

$$-\frac{d[Ru^{VI}]}{dt} = \frac{k}{1 + [H^+]/K_a}[Ru^{VI}][P] \qquad (34)$$

For hypophosphite (P^I), k and K_a are found to be (1.3 ± 0.1) $M^{-1}\,s^{-1}$ and $(9.7 \pm 0.5) \times 10^{-2}\,M$, respectively, at $298.0\,K$ and $I = 1.0\,M$; $\Delta H^{\ddagger}$ and $\Delta S^{\ddagger}$ are $(14.3 \pm 0.5)\,kcal\,mol^{-1}$ and $-(10 \pm 1)\,cal\,mol^{-1}\,K^{-1}$, respectively, at pH 1.86 and $I = 1.0\,M$. For phosphite (P^{III}), k and K_a are found to be $(4.8 \pm 0.4) \times 10^{-2}\,M^{-1}\,s^{-1}$ and $(1.2 \pm 0.2) \times 10^{-2}\,M$, respectively, at $298.0\,K$ and $I = 0.2\,M$; $\Delta H^{\ddagger}$ and $\Delta S^{\ddagger}$ are $(14.1 \pm 1.0)\,kcal\,mol^{-1}$ and $-(18 \pm 3)\,cal\,mol^{-1}\,K^{-1}$, respectively, at pH 2.3 and $I = 0.2\,M$.

For hypophosphite, the kinetic isotope effect, $k(H_2PO_2^-)/k(D_2PO_2^-)$ is 4.1 at pH 1.07 and $I = 1.0\,M$. For phosphite, the kinetic isotopic effect, $k(HDPO_3^-)/k(D_2PO_3^-)$, is 4.0 at pH 2.30 at $I = 0.2\,M$. The large KIEs indicate that the activation process involves P–H bond breaking. A mechanism involving hydride transfer from P–H to $Ru^{VI}=O$ is proposed for these two reactions.

$$H_3PO_X \overset{K_a}{\rightleftharpoons} H_2PO_X^- + H^+ \tag{35}$$

$$[O{=}Ru^{VI}{=}O]^{2+} + H_2PO_X^- \overset{k}{\longrightarrow} [O{=}Ru^{IV}{-}OH]^+ + HPO_X \tag{36}$$

$$HPO_X + H_2O \rightarrow H_3PO_{X+1} \tag{37}$$
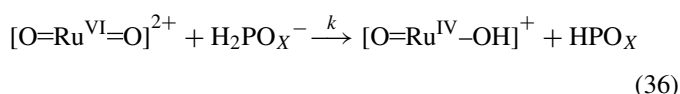
3.7. Oxidation of nitrite [20]

Reaction of *trans*-$[Ru^{VI}(L^1)(O)_2]^{2+}$ with nitrite in aqueous solution or in H_2O/CH_3CN produces the corresponding (nitrato) oxoruthenium(IV) species, *trans*-$[Ru^{IV}(L^1)(O)(ONO_2)]^+$ ($[Ru^{IV}]^+$), which then undergoes relatively slow aquation to give *trans*-$[Ru^{IV}(L^1)(O)(OH_2)]^{2+}$. The stoichiometry for the first and second steps can be represented by Eqs. (38) and (39), respectively.
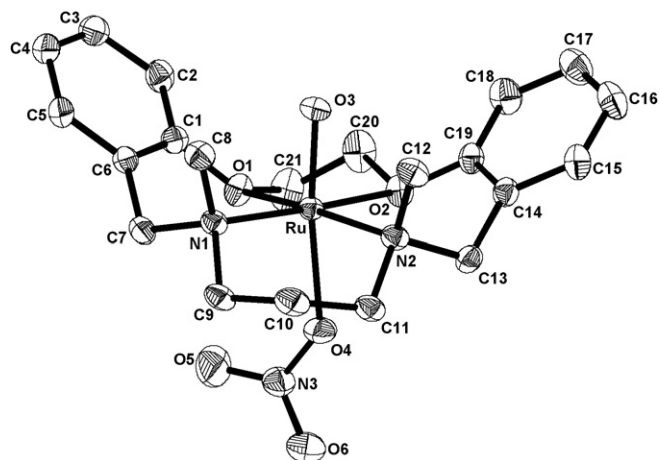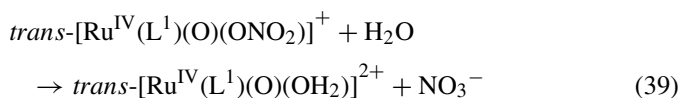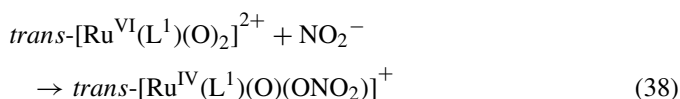
$$trans\text{-}[Ru^{VI}(L^1)(O)_2]^{2+} + NO_2^-$$
$$\rightarrow trans\text{-}[Ru^{IV}(L^1)(O)(ONO_2)]^+ \tag{38}$$

$$trans\text{-}[Ru^{IV}(L^1)(O)(ONO_2)]^+ + H_2O$$
$$\rightarrow trans\text{-}[Ru^{IV}(L^1)(O)(OH_2)]^{2+} + NO_3^- \tag{39}$$

Fig. 2. ORTEP of *trans*-$[Ru^{IV}(L^1)(O)(ONO_2)]^+$, thermal ellipsoids are drawn at the 30% probability (hydrogen atoms are omitted for clarity) [20].

These processes have been monitored by both ESI/MS and UV/vis spectrophotometry. The structure of *trans*-$[Ru^{IV}(L^1)(O)(ONO_2)]^+$ has been determined by X-ray crystallography (Fig. 2). The ruthenium center adopts a distorted octahedral geometry with the oxo and the nitrato ligands *trans* to each other. The Ru=O distance is 1.735(3) Å, the Ru–ONO_2 distance is 2.163(4) Å and the Ru–O–NO_2 angle is 138.46(35)°.

Reaction of *trans*-$[Ru^{VI}(L^1)(^{18}O_2)](ClO_4)_2$ with 1.1 equivalent of $N^{16}O_2^-$ in $H_2^{16}O/CH_3CN$ (1:1, v/v) readily produces the ^{18}O-enriched (nitrato)oxoruthenium(IV) complex *trans*-$[Ru^{IV}(L^1)(^{18}O)(^{18}ONO_2)]ClO_4$. The ESI/MS spectrum of *trans*-$[Ru^{IV}(L^1)(^{18}O)(^{18}ONO_2)]ClO_4$ taken 5 min after dissolution in 1 mM CF_3COOH in H_2O/CH_3CN (1:1, v/v) shows the most abundant peak at $m/z = 524$ $[Ru^{IV}{-}^{18}O_2]^+$ (i.e. the parent ion with two ^{18}O atoms). Analysis of the $[Ru^{IV}{-}^{18}O_2]^+$ cluster (Fig. 3) indicates that although there are on the average two ^{18}O atoms per ion, the actual isotopic composition is 30% $[Ru^{IV}{-}^{18}O^{16}O]^+$, 40% $[Ru^{IV}{-}^{18}O_2]^+$ and 30% $[Ru^{IV}{-}^{18}O_3]^+$ (each $\pm 5\%$). On standing the peak at $m/z = 524$ gradually decreases while the peak at $m/z = 477$ {*trans*-$[Ru^{IV}(L^1)(^{18}O)(^{16}OH_2)]^{2+}$} increases, indicating aquation of $[Ru^{IV}{-}^{18}O_2]^+$ to give *trans*-$[Ru^{IV}(L^1)(^{18}O)(^{16}OH_2)]^{2+}$. The $t_{1/2}$ for this aquation is ca. 30 min at 297 K. Notably, although the intensities of the two peaks vary with time, the iso-

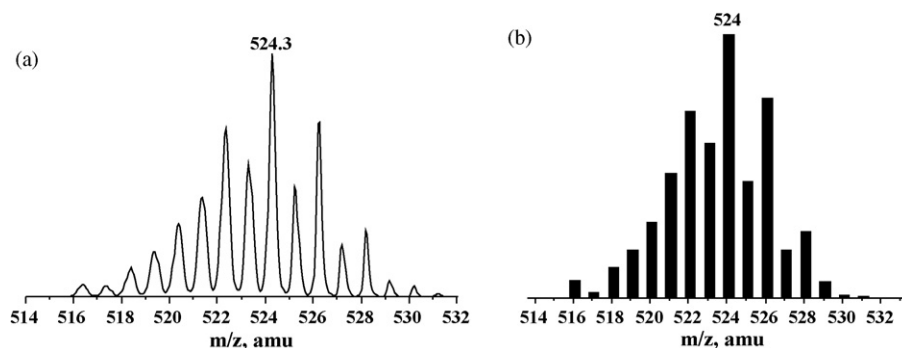Fig. 3. (a) Expanded isotopic distribution of the cluster at $m/z = 524$ in the ESI/MS spectrum of $[Ru^{IV}]ClO_4$-$^{18}O_2$. (b) Simulated isotopic pattern for 30% $[Ru^{IV}]$-^{18}O, 40% $[Ru^{IV}]$-$^{18}O_2$ and 30% $[Ru^{IV}]$-$^{18}O_3$ [20].
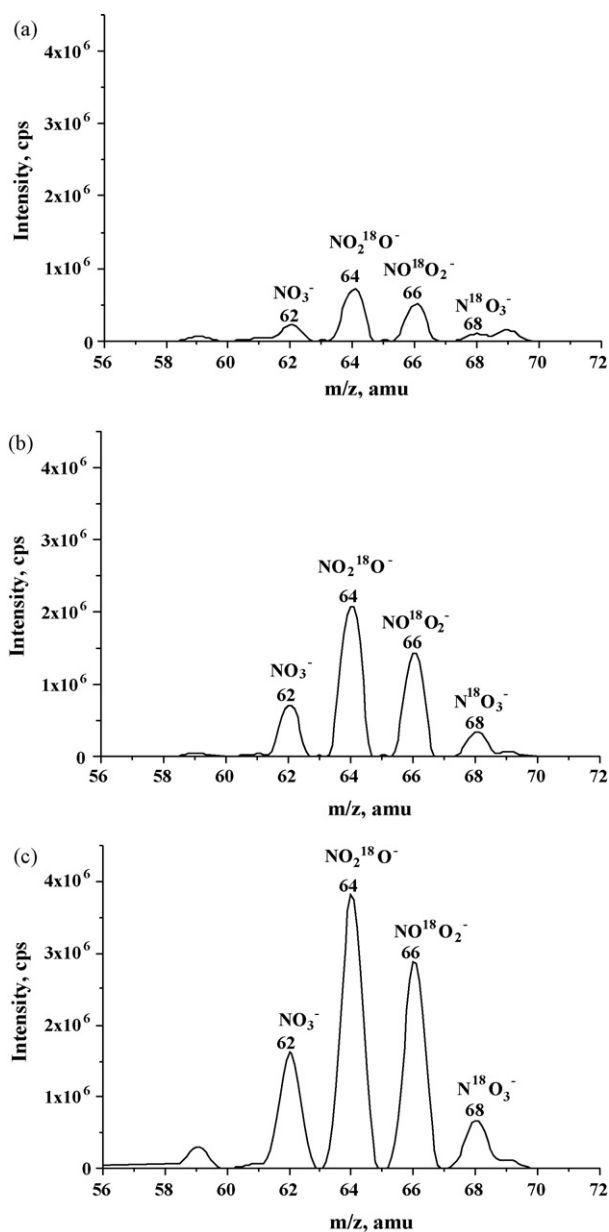
Fig. 4. ESI/MS spectra (−ve mode) of [Ru^{IV}]ClO$_4$-^{18}O$_2$ in 1 mM of CF$_3$COOH in H$_2$O/CH$_3$CN (1:1, v/v) at different time intervals, (a) 5 min; (b) 30 min; (c) 120 min [20].

topic distributions remain unchanged. This means that there is no O-exchange between [Ru^{IV}-^{18}O$_2$]$^+$ and H$_2$^{16}O, and between the oxo ligand in *trans*-[Ru^{IV}(L^1)(^{18}O)(^{16}OH$_2$)]$^{2+}$ and H$_2$^{16}O during this period (2 h, 297 K).
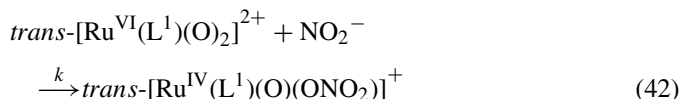
The nitrate released during the aquation of [Ru^{IV}-^{18}O$_2$]$^+$ is shown to be quantitative by ion chromatography. It was also monitored by ESI/MS in the negative mode. Fig. 4 shows the ESI/MS spectra (−ve mode) of [Ru^{IV}]ClO$_4$-^{18}O$_2$ at various time-intervals after dissolution in 1 mM CF$_3$COOH in H$_2$O/CH$_3$CN (1:1, v/v). Notably N^{16}O$_3$$^-$ (*m/z* = 62), N^{18}O^{16}O$_2$$^-$ (*m/z* = 64), N^{18}O$_2$^{16}O$^-$ (*m/z* = 66) and N^{18}O$_3$$^-$ (*m/z* = 68) are all detected. The intensities of all these peaks increase with time, consistent with the release of nitrate during aquation of [Ru^{IV}-^{18}O$_2$]$^+$. The $t_{1/2}$ is ca. 30 min at 297 K,

in agreement with the result obtained from monitoring [Ru^{IV}-^{18}O$_2$]$^+$ in the positive mode. Significantly the *relative* intensities of the four peaks remain more or less unchanged, and assuming that the relative intensities of the peaks are equal to the relative amounts of the respective ions, then the average % of N^{16}O$_3$$^-$, N^{18}O^{16}O$_2$$^-$, N^{18}O$_2^{16}O^-$ and N^{18}O$_3$$^-$ = 14, 41, 38 and 7, respectively, (each ± 5%). If random scrambling of the ^{18}O atoms has occurred in the initially formed *trans*-[Ru^{IV}(L^1)(^{18}O)(^{18}ONO$_2$)]$^+$ prior to aquation, as described for the [Ru^{IV}-^{18}O$_2$]$^+$ species, then the % should be 12.5, 37.5, 37.5 and 12.5, respectively, which is in reasonable agreement with the observed values. Independent experiments indicate that there is no O-exchange between both NaNO$_3$ and NaNO$_2$ with H$_2$^{18}O under similar conditions.

The kinetics for the first step (Eq. (38)) have also been studied in aqueous acidic solution. The rate is first order in both [Ru^{VI}] and [NO$_2$$^-$], the second-order rate constant k_2 increases with pH (1–3) according to the relationship shown below:

$$k_2 = \frac{k}{1 + [H^+]/K_a} \tag{40}$$

K_a is the acid dissociation constant of nitrous acid, k and K_a are found to be $(2.33 \pm 0.15) \times 10^4 \, M^{-1} \, s^{-1}$ and $(9.10 \pm 0.90) \times 10^{-4} \, M$, respectively. The observed acid dependence of k_2 is consistent with the reaction scheme shown in Eqs. (41) and (42).

$$HNO_2 \overset{K_a}{\rightleftharpoons} NO_2^- + H^+ \tag{41}$$

$$\textit{trans-}[Ru^{VI}(L^1)(O)_2]^{2+} + NO_2^-$$
$$\overset{k}{\longrightarrow} \textit{trans-}[Ru^{IV}(L^1)(O)(ONO_2)]^+ \tag{42}$$

The value of K_a is in good agreement with the literature value of $K_a = 1.1 \times 10^{-3} \, M$ [16]. At pH 2.92 and $I = 0.1 \, M$, $\Delta H^{\ddagger}$ and $\Delta S^{\ddagger}$ are found to be $(4.2 \pm 0.2) \, kcal \, mol^{-1}$ and $-(26 \pm 3) \, cal \, mol^{-1} \, K^{-1}$, respectively. By using the Marcus cross-relation, k_{12} is calculated to be $2.4 \times 10 \, M^{-1} \, s^{-1}$ at 298 K, which is almost three orders of magnitude slower than the experimental rate constant.
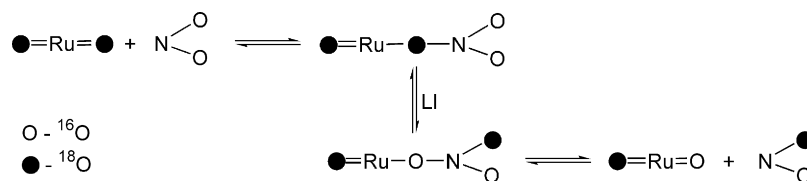
A reversible OAT mechanism is proposed to account for the scrambling of the ^{18}O atoms, as shown in Scheme 2.

The proposed mechanism starts with oxygen-atom transfer to produce initially *trans*-[Ru^{IV}(L^1)(^{18}O)(^{18}ONO$_2$)]$^+$. This species then undergoes rapid linkage isomerisation (LI) through rotation of the nitrato ligand. This is followed by back oxygen-atom transfer to generate singly ^{18}O-labeled *trans*-[Ru^{VI}(L^1)(^{18}O)(^{16}O)]$^{2+}$ and N^{18}O^{16}O$^-$ ions. Repetition of these processes would result in the observed scrambling of the ^{18}O atoms in the (nitrato)oxoruthenium(VI) species.

4. Oxidation of organic substrates

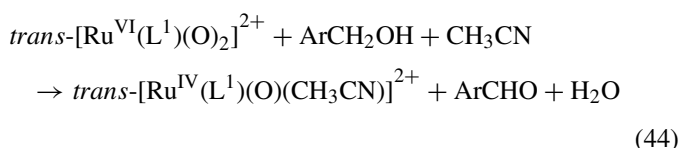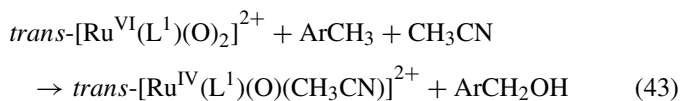### 4.1. Oxidation of alkylaromatic compounds [21]

The oxidation of a series of 21 alkylaromatic compounds by *trans*-[Ru^{VI}(L^1)(O)$_2$]$^{2+}$ has been studied in CH$_3$CN. The major

Scheme 2.

reaction pathways occurring in the oxidation of alkylaromatic compounds with primary or secondary C–H bonds by *trans*-[Ru^{VI}(L^1)(O)$_2$]$^{2+}$ can be represented by Eqs. (43) and (44).

$$trans\text{-}[Ru^{VI}(L^1)(O)_2]^{2+} + ArCH_3 + CH_3CN$$
$$\rightarrow trans\text{-}[Ru^{IV}(L^1)(O)(CH_3CN)]^{2+} + ArCH_2OH \quad (43)$$

$$trans\text{-}[Ru^{VI}(L^1)(O)_2]^{2+} + ArCH_2OH + CH_3CN$$
$$\rightarrow trans\text{-}[Ru^{IV}(L^1)(O)(CH_3CN)]^{2+} + ArCHO + H_2O$$
$$(44)$$

The initial product is the alcohol, which is then further oxidized to the corresponding aldehyde or ketone. The carbonyl compound is the major product because in general alcohols are oxidized much more rapidly than hydrocarbons by *trans*-[Ru^{VI}(L^1)(O)$_2$]$^{2+}$ [5,22].

The kinetics of the reactions have been monitored by UV–vis spectrophotometry, and the rate law is:

$$-\frac{d[Ru^{VI}]}{dt} = k_2[Ru^{VI}][ArCH_3] \quad (45)$$

The rate constant k_2 for various substrates together with the activation parameters are compiled in Table 1. The KIEs for the oxidation of toluene/d_8-toluene and fluorene/d_{10}-fluorene are 15 and 10.5, respectively, at 298.0 K.

A plot of $\Delta H^{\ddagger}$ versus $\Delta S^{\ddagger}$ is linear (Fig. 5), suggesting that all the hydrocarbons react by a common mechanism. A good linear correlation between $\Delta G^{\ddagger}$ and ΔH° is also found (Fig. 6), which

strongly supports a HAT mechanism for the oxidation of these substrates by *trans*-[Ru^{VI}(L^1)(O)$_2$]$^{2+}$ [23]. ΔH° is the difference between the strength of the bond being broken and that being formed in a H-atom transfer step, i.e. ΔH° = BDE of ArCH$_2$-H − BDE of [O=Ru^V(L^1)O-H]$^{2+}$. BDE of [O=Ru^V(L^1)O-H]$^{2+}$ has been calculated to be 82.8 kcal mol^{-1} [24]. $\Delta H^{\ddagger}$ also correlates with ΔH° since $\Delta H^{\ddagger}$ is proportional to $\Delta S^{\ddagger}$. Recently a variety of H-atom transfer reactions have been shown to follow the Marcus cross-relation [25]. The observation of a linear correlation between $\Delta G^{\ddagger}$ and ΔH° in this case means that the H-atom self-exchange rates of the alkylaromatics are similar. The slope of (0.61 ± 0.06) in the $\Delta G^{\ddagger}/\Delta H^{\circ}$ plot is in reasonable agreement with the theoretical slope of 0.5 predicted by the Marcus theory (for $\Delta G^{\circ} \sim 0$, and assuming $\Delta H^{\circ} \sim \Delta G^{\circ}$).

The rate constants for H-atom abstraction from various alkylaromatic compounds by *trans*-[Ru^{VI}(L^1)(O)$_2$]$^{2+}$ also correlate with the rates of abstraction by ^{t}BuOO$^\bullet$, ^{t}BuO$^\bullet$ and MnO$_4^-$, plots of log k_2' (per active hydrogen of the substrates) versus the strength of the O–H bond formed by the oxidants are roughly linear (Fig. 7). Such a correlation is typical for HAT reactions [26].

Using the Marcus cross-relation, it is possible to estimate the [Ru^{VI}(L^1)(O)$_2$]$^{2+}$/[Ru^V(L^1)(O)(OH)]$^{2+}$ self-exchange rate. The self-exchange rate for PhCH$_3$/PhCH$_2$$^\bullet$ is reported to be $\sim 4 \times 10^{-5}$ M^{-1} s^{-1} at 298 K [25]. ΔG° for the reaction between Ru^{VI} and PhCH$_3$ is evaluated using the equation: $\Delta G^{\circ} = \Delta H^{\circ}$ = BDE of PhCH$_2$-H − BDE of [O=Ru^V(L^1)O-H]$^{2+}$ = (89.8 − 82.8) = 7 kcal mol^{-1}. The rate constant for the cross-reaction is 1.11×10^{-4} M^{-1} s^{-1} at 298 K. Using these
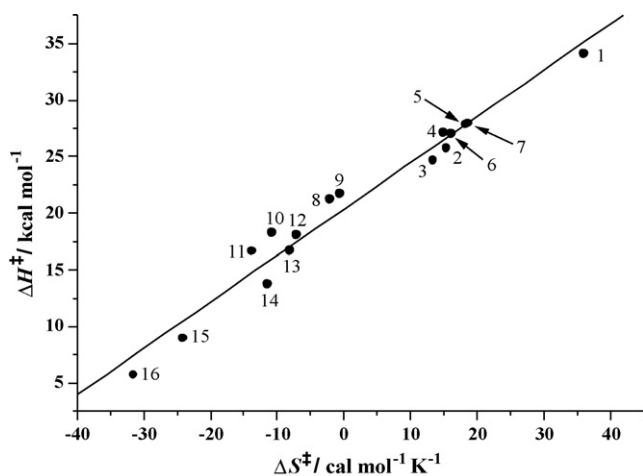
Fig. 5. Plot of $\Delta H^{\ddagger}$ vs. $\Delta S^{\ddagger}$ for the oxidation of alkylaromatic compounds by *trans*-[Ru^{VI}(L^1)(O)$_2$]$^{2+}$ in CH$_3$CN (the numberings in the plot are defined in Table 1) [21].
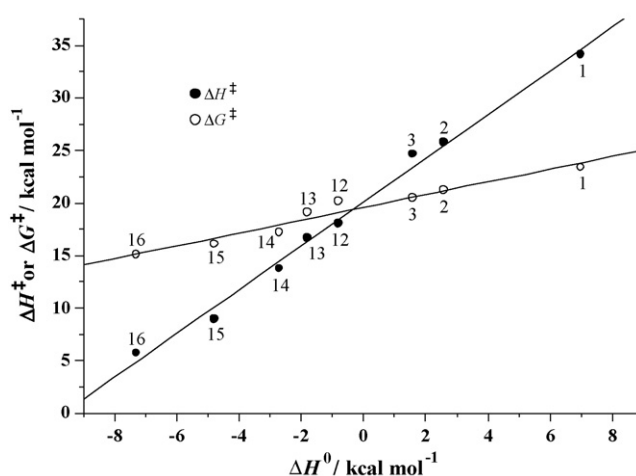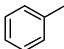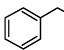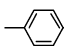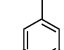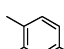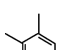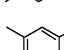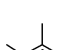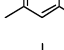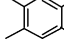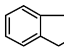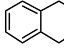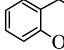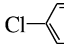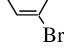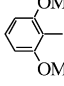
Fig. 6. Plot of $\Delta H^{\ddagger}$ and $\Delta G^{\ddagger}$ vs. ΔH° for the HAT step in the oxidation of alkylaromatic compounds by *trans*-[Ru^{VI}(L^1)(O)$_2$]$^{2+}$ in CH$_3$CN at 298 K (the numberings in the plot are defined in Table 1) [21].
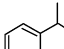
Table 1
Second-order rate constants at 298.0 K and activation parameters for the oxidation of alkylaromatic compounds by trans-[Ru^{VI}(L^1)(O)$_2$]$^{2+}$ [21]

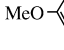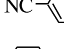| No.	Substrate	k_2 (M^{-1} s^{-1})[a]	$\Delta H^{\ddagger}$ [b] (kcal mol^{-1})	$\Delta S^{\ddagger}$ [b] (cal K^{-1} mol^{-1})	BDE[c] (kcal mol^{-1})	E° [d] [V(NHE)]
1	*(structure)*	$(3.70 \pm 0.13) \times 10^{-5}$, $(6.63 \pm 0.07) \times 10^{-5e}$	34.1 ± 1.4	36 ± 5	89.8	2.64
2	*(structure)*	$(1.82 \pm 0.05) \times 10^{-3}$	25.7 ± 0.6	15 ± 2	85.4	2.62
3	*(structure)*	$(5.38 \pm 0.03) \times 10^{-3}$	24.7 ± 0.8	14 ± 2	84.4	2.53
4	*(structure)*	$(1.62 \pm 0.03) \times 10^{-4}$	27.1 ± 1.9	15 ± 3		2.30
5	*(structure)*	$(2.19 \pm 0.01) \times 10^{-4}$	27.8 ± 0.7	18 ± 2		2.35
6	*(structure)*	$(3.01 \pm 0.07) \times 10^{-4}$	27.1 ± 1.0	16 ± 3		2.13
7	*(structure)*	$(2.19 \pm 0.02) \times 10^{-4}$	27.9 ± 0.7	19 ± 2		2.23
8	*(structure)*	$(6.29 \pm 0.19) \times 10^{-4}$	21.2 ± 1.5	$-(2 \pm 2)$		1.94
9	*(structure)*	$(5.56 \pm 0.03) \times 10^{-4}$	21.7 ± 1.0	$-(1 \pm 2)$		1.95
10	*(structure)*	$(1.13 \pm 0.07) \times 10^{-3}$	18.3 ± 0.9	$-(11 \pm 2)$		1.87
11	*(structure)*	$(3.75 \pm 0.04) \times 10^{-3}$	16.6 ± 0.3	$-(14 \pm 2)$		1.74
12	Ph$_2$CH$_2$	$(1.03 \pm 0.03) \times 10^{-2}$	18.0 ± 1.3	$-(7 \pm 2)$	82.0	
13	Ph$_3$CH	$(6.20 \pm 0.06) \times 10^{-2}$	16.7 ± 1.2	$-(8 \pm 2)$	81.0	
14	*(fluorene)*	1.58 ± 0.03	13.8 ± 0.5	$-(11 \pm 2)$	80.1	1.91
15	*(anthracene/dihydroanthracene)*	7.45 ± 0.15	9.0 ± 1.2	$-(24 \pm 3)$	78.0	1.94
16	*(xanthene)*	49.7 ± 0.4	5.7 ± 0.9	$-(32 \pm 3)$	75.5	
17	Cl—*(structure)*—	$(1.62 \pm 0.07) \times 10^{-3e}$				
18	MeO—*(structure)*—	$(2.89 \pm 0.03) \times 10^{-3e}$				
19	NC—*(structure)*—	$(1.17 \pm 0.03) \times 10^{-2e}$				
20	*(structure, Br)*	$(2.29 \pm 0.04) \times 10^{-5e}$				
21	*(structure, OMe, OMe)*	$(8.27 \pm 0.11) \times 10^{-6e}$				

[a] Values are at 298 K and corrected per active hydrogen of the substrates.
[b] Temperature range 288–328 K.
[c] Data are from reference [40].
[d] Data are from reference [41].
[e] Value at 313.0 K and corrected per active hydrogen of the substrate.

Fig. 7. Plot of $\log k_2'$ (the rate constant for H-atom abstraction, per H-atom) vs. the strength of the O–H bond formed by the oxidants. Solid line (DHA), dash line (Ph$_2$CH$_2$), dot line (PhEt), and dash-dot line (PhMe) [21].
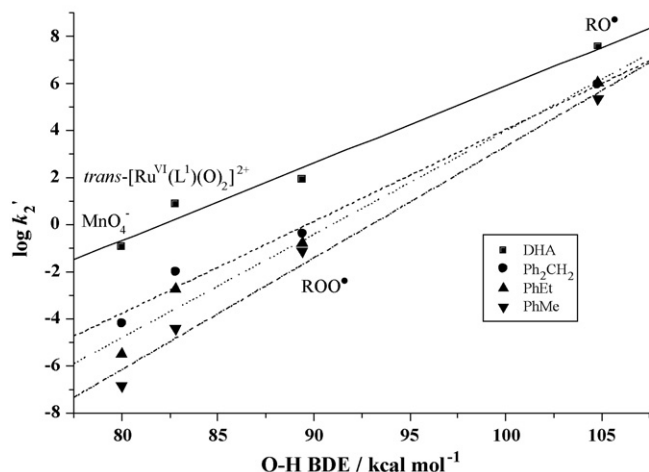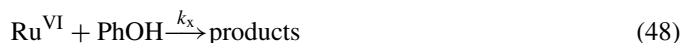
data the $[Ru^{VI}(L^1)(O)_2]^{2+}/[Ru^V(L^1)(O)(OH)]^{2+}$ self-exchange rate in CH$_3$CN is estimated to be 2×10^1 M^{-1} s^{-1} at 298 K.

4.2. Oxidation of phenols [24]

The kinetics of the oxidation of phenols by *trans*-$[Ru^{VI}(L^1)(O)_2]^{2+}$ have been studied in aqueous acidic solutions and in CH$_3$CN. In H$_2$O the oxidation of phenol produces the unstable 4,4′-biphenoquinone, as evidenced by a rapid increase and then a slow decrease in absorbance at 398 nm. The first step (i.e. the increase in absorbance) is first-order in both Ru^{VI} and phenol, and the rate constant k_f depends on [H$^+$] according to Eq. (46).

$$k_f = k_x + \left(\frac{k_y K_a}{[H^+]} \right) \tag{46}$$

This is consistent with the following scheme:

$$\text{PhOH} \overset{K_a}{\rightleftharpoons} \text{PhO}^- + \text{H}^+ \tag{47}$$

$$\text{Ru}^{VI} + \text{PhOH} \xrightarrow{k_x} \text{products} \tag{48}$$

$$\text{Ru}^{VI} + \text{PhO}^- \xrightarrow{k_y} \text{products} \tag{49}$$

At 298 K and $I = 0.1$M, $k_x = (1.25 \pm 0.10) \times 10$ M^{-1} s^{-1} and $k_y = (7.96 \pm 0.16) \times 10^8$ M^{-1} s^{-1}. For the k_x step, $\Delta H^{\ddagger} = (11.3 \pm 0.8)$ kcal mol^{-1} and $\Delta S^{\ddagger} = -(14 \pm 3)$ cal mol^{-1} K^{-1}. For the k_y step, $\Delta H^{\ddagger} = (10.0 \pm 0.5)$ kcal mol^{-1} and $\Delta S^{\ddagger} = (15 \pm 2)$ cal mol^{-1} K^{-1}.

At $I = 0.1$ M and pH 2.98, the KIEs are $k(H_2O)/k(D_2O) = 4.8$ and 0.74 for k_x and k_y, respectively, and $k_f(C_6H_5OH)/k_f(C_6D_5OH) = 1.1$. It is proposed that the k_x step, i.e. oxidation of PhOH, occurs by a hydrogen atom abstraction mechanism; while the k_y step, i.e. the oxidation of PhO$^-$, occurs by an electron-transfer mechanism. In both steps the phenoxy radical is produced, which then undergoes two rapid concurrent reactions. One is a further three-electron oxidation by Ru^{VI} and Ru^V to give *p*-benzoquinone and other organic products, the other one is a coupling and oxidation process to give 4,4′-biphenoquinone, followed by the decay step, k_s. The proposed mechanism is shown in Scheme 3.

The oxidation of various substituted phenols were also investigated at pH 1.1. At this pH the pathway involving oxidation of the phenolate anion is insignificant, and $k_f \approx k_x$. The spectrophotometric changes for the oxidation of *ortho* substituted phenols show the same biphasic behavior as for the parent phenol. However, for *meta* and *para* substituted phenols no intermediate formation of the highly absorbing 4,4′-biphenoquinone derivatives are observed. Instead the spectral changes reveal only decay of *trans*-$[Ru^{VI}(L^1)(O)_2]^{2+}$ ($\lambda_{max} = 385$ nm) to *trans*-$[Ru^{IV}(L^1)(O)(OH_2)]^{2+}$. For the *meta* and *para* substituted phenols the decay at 385 nm follows first-order kinetics and
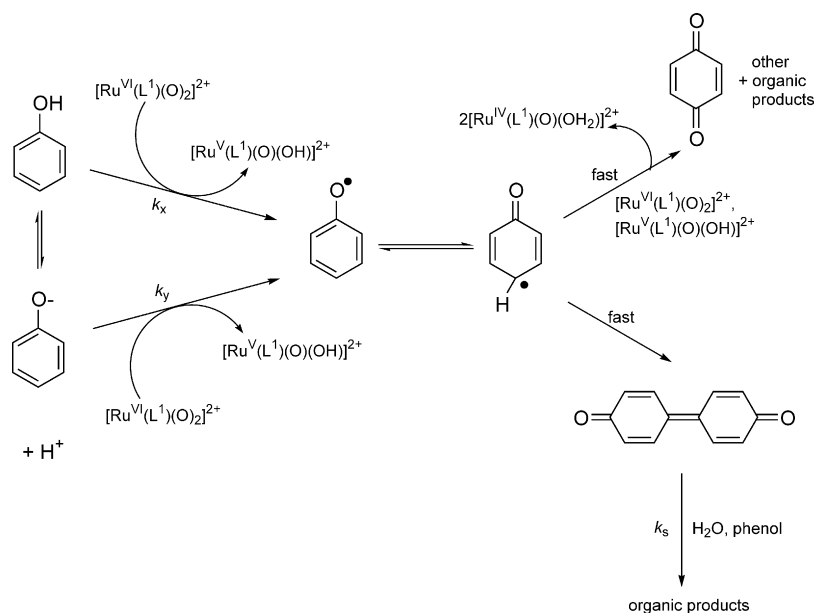
Scheme 3.

Table 2
Second-order rate constants for the oxidation of substituted phenols (X-PhOH) by *trans*-[Ru^{VI}(L^1)(O)$_2$]$^{2+}$ in H$_2$O (pH 1.10, $I = 0.1$ M) and CH$_3$CN at 298.0 K [24]

X	O–H BDE (kcal mol^{-1})	k_x(H$_2$O) (M^{-1} s^{-1})	k_x(CH$_3$CN) (M^{-1} s^{-1})
H	87.05	$(1.10 \pm 0.04) \times 10$	2.36 ± 0.09
2-Me	85.05	$(1.38 \pm 0.04) \times 10^2$	$(1.66 \pm 0.06) \times 10$
3-Me	86.65	$(2.32 \pm 0.05) \times 10$	9.46 ± 0.08
3-CF3	89.15	$(5.69 \pm 0.10) \times 10^{-1}$	$(4.17 \pm 0.11) \times 10^{-1}$
3-CN	89.75	$(2.00 \pm 0.07) \times 10^{-1}$	$(1.19 \pm 0.06) \times 10^{-1}$
4-MeO	80.95	$(8.94 \pm 0.22) \times 10^4$	$(3.06 \pm 0.06) \times 10^3$
4-Me	84.58	$(1.89 \pm 0.03) \times 10^2$	$(1.25 \pm 0.04) \times 10$
4-*t*-Bu	84.76	$(1.36 \pm 0.04) \times 10^2$	$(1.89 \pm 0.03) \times 10$
4-Cl	85.65	$(1.87 \pm 0.05) \times 10$	7.77 ± 0.20
4-CN	89.25	$(8.03 \pm 0.21) \times 10^{-2}$	$(2.23 \pm 0.07) \times 10^{-1}$
2-Cl-4-Me	85.55		$(1.84 \pm 0.05) \times 10$
2,4-Di-*t*-Bu	81.85		$(1.35 \pm 0.02) \times 10^2$
3,5-Di-*t*-Bu	85.68		7.54 ± 0.10
2,6-Di-*t*-Bu	81.65		$(5.80 \pm 0.08) \times 10^{-1}$
2,6-Di-*t*-Bu-4-Me	79.15		$(2.63 \pm 0.09) \times 10$
2,6-Di-*t*-Bu-4-MeO	75.55		$(2.56 \pm 0.07) \times 10^{-4}$

the pseudo-first-order rate constants depend linearly on [PhOH]. Representative second-order rate constants are shown in Table 2.

Similar kinetic behavior is also observed for reactions in acetonitrile. The small KIE of 1.1 for the oxidation of C$_6$H$_5$OH versus C$_6$D$_5$OH, and the reactivity order of *ortho* ≈ *para* > *meta* for the oxidation of methylphenols suggest that a similar hydrogen atom abstraction mechanism for the oxidation of phenols occurs in CH$_3$CN as in H$_2$O. The phenoxyl radical produced either undergoes coupling or is further oxidized by the ruthenium oxo species.

Hammett plots of $\log(k_x^X / k_x^H)$ against σ^+ are reasonably linear for reactions in H$_2$O and in CH$_3$CN (Fig. 8), with the slopes $\rho = -(3.76 \pm 0.30)$ and $-(2.90 \pm 0.25)$, respectively. The negative reaction constants are consistent with the formation of the electron-deficient phenoxyl radical intermediate. A good correlation between rate constants and σ^+ has also been observed for hydrogen abstraction of phenols by *tert*-butyl radicals [27].

For reaction in aqueous solutions there is a linear correlation between log(rate constant) at 298 K and the O–H BDE of a series of mono-substituted phenols that do not contain any bulky substituents in the *ortho* positions (Fig. 9a). For the same plot in CH$_3$CN (Fig. 9b), it is found that phenols without any bulky *tert*-butyl substituent in the *ortho* positions fall on one straight line. However, phenols that contain 2,6-di-*tert*-butyl groups react much more slowly than phenols of similar O–H BDE but with no such bulky groups, and they fall on a separate line in the plot, while 2,4-di-*tert*-butylphenol lies between the two lines. Evidently steric crowding about the hydroxyl group is very important in affecting the reactivity of the phenols, which is expected for a hydrogen atom abstraction mechanism but not for an electron-transfer mechanism. Similar steric effects have been observed in hydrogen atom abstraction from phenols by peroxy radicals [28] and alkyl radicals [29]. A reasonably linear correlation is also found between log k_x (the rate constant for hydrogen atom abstraction from phenol) and the strength of the O–H bond formed for a number of oxygen radicals [30,31] and *trans*-[Ru^{VI}(L^1)(O)$_2$]$^{2+}$ (Fig. 10).

4.3. Oxidation of hydroquinones [32]

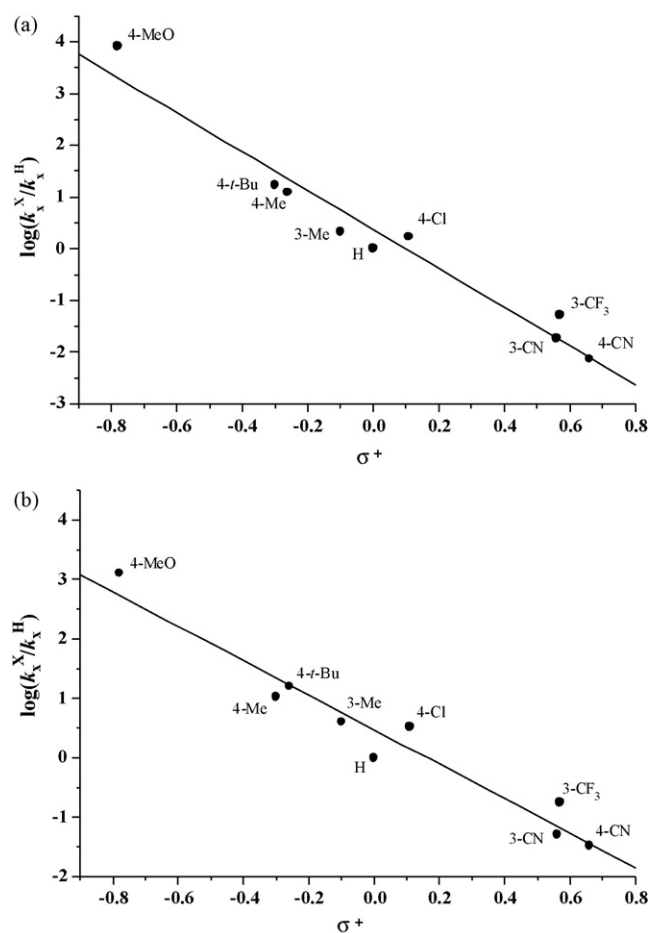The kinetics of the oxidation of a series of hydroquinones in both aqueous solutions and CH$_3$CN by *trans*-[Ru^{VI}(L^2)(O)$_2$]$^{2+}$ have been studied.

Fig. 8. Hammett plot of $\log(k_x^X / k_x^H)$ vs. σ^+ for the oxidation of substituted phenols by *trans*-[Ru^{VI}(L^1)(O)$_2$]$^{2+}$ at 298.0 K: (a) in H$_2$O (pH 1.10 and $I = 0.1$ M) and (b) in CH$_3$CN [24].
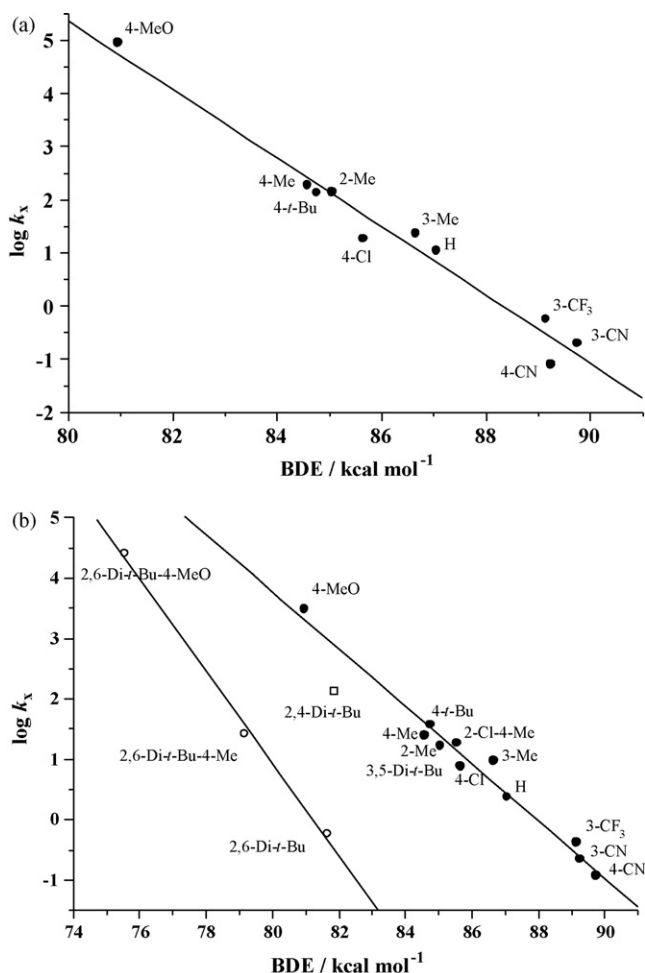
Fig. 9. Plot of $\log k_x$ vs. O–H BDE for the oxidation of phenols by *trans*-$[Ru^{VI}(L^1)(O)_2]^{2+}$ at 298.0 K: (a) in H_2O (pH 1.10 and $I = 0.1$ M) and (b) in CH_3CN [24].
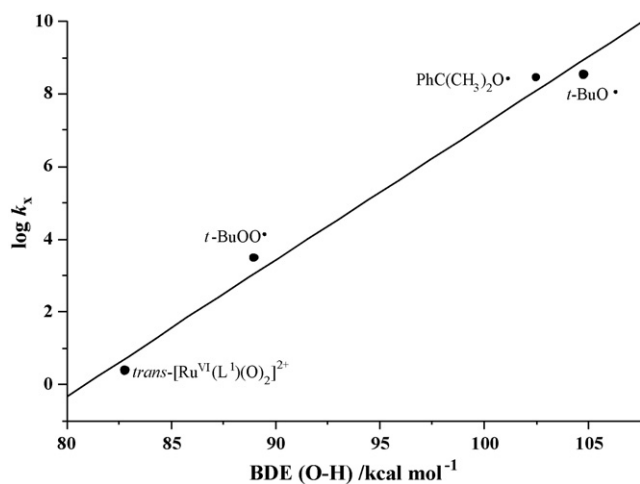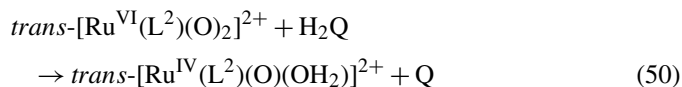

Fig. 10. Plot of log(rate constants) at 298 K for hydrogen atom abstraction of phenol by oxygen radicals and *trans*-$[Ru^{VI}(L^1)(O)_2]^{2+}$ vs. the strength of the O–H bond [24].

In aqueous solutions the stoichiometry is:

$$trans\text{-}[Ru^{VI}(L^2)(O)_2]^{2+} + H_2Q$$
$$\rightarrow trans\text{-}[Ru^{IV}(L^2)(O)(OH_2)]^{2+} + Q \tag{50}$$

The following rate law is obtained:

$$-\frac{d[Ru^{VI}]}{dt} = \frac{k_a[H^+] + k_b K_a}{[H^+] + K_a}[Ru^{VI}][H_2Q] \tag{51}$$

K_a is the acid dissociation constant of H_2Q and is taken as 1.41×10^{-10} M at 298.0 K [33]. At 298.0 K and $I = 0.1$ M, k_a and k_b are $(9.41 \pm 0.28) \times 10^1$ and $(7.91 \pm 0.10) \times 10^7$ M^{-1} s^{-1}, respectively. At pH 1.16 and $I = 0.1$ M $\Delta H^{\ddagger}$ and $\Delta S^{\ddagger}$ are found to be (12.3 ± 0.1) kcal mol^{-1} and $-(8 \pm 1)$ cal mol^{-1} K^{-1}, respectively. The observed rate law is consistent with parallel pathways involving oxidation of H_2Q and HQ^- (Eqs. (52)–(54)):

$$H_2Q \underset{K_a}{\rightleftharpoons} HQ^- + H^+ \tag{52}$$

$$Ru^{VI} + H_2Q \xrightarrow{k_a} products \tag{53}$$

$$Ru^{VI} + HQ^- \xrightarrow{k_b} products \tag{54}$$

In aqueous solutions at pH 1.79, where the pathway involving the oxidation of HQ^- is insignificant, a large KIE for the oxidation of H_2Q in D_2O $\{k(H_2O)/k(D_2O) = 4.9\}$ is observed. However, no KIE is found for the oxidation of H_2Q-d_4 in H_2O, $k\{C_6H_4(OH)_2\}/k\{C_6D_4(OH)_2\} = 1.0$. These results suggest that the rate-determining step for the oxidation of the H_2Q molecule involves O–H bond cleavage. On the other hand, at pH 4.60, in which the oxidation of the HQ^- anion is the predominant pathway, a negligible KIE of 1.2 ± 0.2 is found for the oxidation of H_2Q in D_2O, suggesting that in this case a simple outer-sphere electron-transfer mechanism is operating.

The mechanism for the oxidation of H_2Q by *trans*-$[Ru^{VI}(L^2)(O)_2]^{2+}$ in aqueous acidic solution (pH < 3) is summarized in Eqs. (55)–(59).

$$trans\text{-}[Ru^{VI}(L^2)(O)_2]^{2+} + H_2Q$$
$$\xrightarrow{slow} trans\text{-}[Ru^V(L^2)(O)(OH)]^{2+} + HQ^{\bullet} \tag{55}$$

$$trans\text{-}[Ru^{VI}(L^2)(O)_2]^{2+} + HQ^{\bullet}$$
$$\xrightarrow{fast} trans\text{-}[Ru^V(L^2)(O)(OH)]^{2+} + Q \tag{56}$$

$$trans\text{-}[Ru^V(L^2)(O)(OH)]^{2+} + H_2Q$$
$$\xrightarrow{fast} trans\text{-}[Ru^{IV}(L^2)(O)(OH_2)]^{2+} + HQ^{\bullet} \tag{57}$$

$$trans\text{-}[Ru^V(L^2)(O)(OH)]^{2+} + HQ^{\bullet}$$
$$\xrightarrow{fast} trans\text{-}[Ru^{IV}(L^2)(O)(OH_2)]^{2+} + Q \tag{58}$$

$$2HQ^{\bullet} \xrightarrow{fast} H_2Q + Q \tag{59}$$
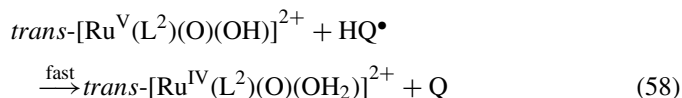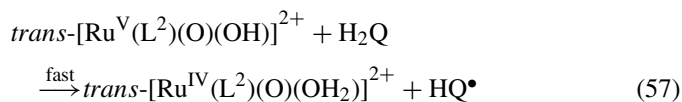
Table 3
Second-order rate constants for the oxidation of H$_2$Q-X by *trans*-[Ru^{VI}(L^2)(O)$_2$]$^{2+}$ in both aqueous solutions and acetonitrile at 298.0 K [32]

Substrate	k_{H_2O} (M^{-1} s^{-1})[a]	k_{ACN} (M^{-1} s^{-1})[c]	k'_{ACN} (M^{-1} s^{-1})[c]
2,5-Di-^{t}Bu	$(5.62 \pm 0.05) \times 10^2$	$(2.51 \pm 0.17) \times 10^2$	$(1.00 \pm 0.09) \times 10^1$
^{t}Bu	$(7.21 \pm 0.15) \times 10^2$	$(3.50 \pm 0.52) \times 10^2$	$(1.18 \pm 0.05) \times 10^1$
2,3-Di-Me	$(6.60 \pm 0.02) \times 10^2$	$(2.90 \pm 0.14) \times 10^2$	$(1.13 \pm 0.04) \times 10^1$
Me	$(6.05 \pm 0.04) \times 10^2$	$(2.24 \pm 0.06) \times 10^2$	8.44 ± 0.13
OMe	$(3.18 \pm 0.03) \times 10^2$	$(1.73 \pm 0.08) \times 10^2$	5.40 ± 0.14
H	$(9.37 \pm 0.12) \times 10^1$	$(8.53 \pm 0.32) \times 10^1$	2.21 ± 0.04
Cl	$(5.19 \pm 0.06) \times 10^1$	$(3.44 \pm 0.16) \times 10^1$	1.49 ± 0.06
2,3-Di-CN	1.27 ± 0.07[b]	1.00 ± 0.04	$(4.70 \pm 0.07) \times 10^{-2}$

[a] Experiments were carried out in aqueous solution at pH 1.8 and $I = 0.1$ M unless specified.
[b] Experiment was carried out at pH 1.0.
[c] Experiments were carried out in CH$_3$CN. k_{ACN} and k'_{ACN} are the rate constants for the first and second steps, respectively, (Eqs. (60) and (61)).
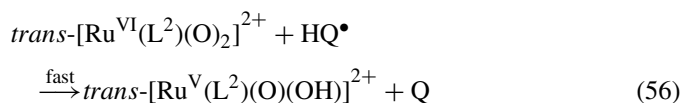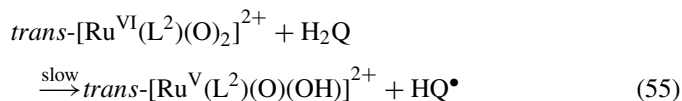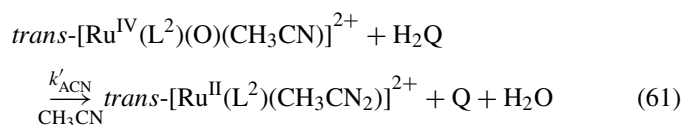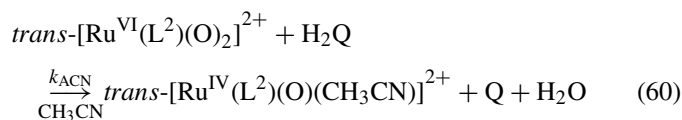
HQ$^\bullet$ is known to disproportionate rapidly ($k = 1.1 \times 10^9$ M^{-1} s^{-1}) [34].

In contrast to reaction in water, the spectrophotometric changes for the oxidation of H$_2$Q by *trans*-[Ru^{VI}(L)(O)$_2$]$^{2+}$ CH$_3$CN indicate biphasic behavior. The final spectrum (after removal of organics) shows quantitative formation of *trans*-[Ru^{II}(L^2)(CH$_3$CN)$_2$]$^{2+}$ [35]. The spectrophotometric changes for the second step are identical to that for the reaction of H$_2$Q with *trans*-[Ru^{IV}(L^2)(O)(CH$_3$CN)]$^{2+}$. Also 2 mol *p*-benzoquinone are formed from 1 m of Ru^{VI}. Thus, the reaction of *trans*-[Ru^{VI}(L^2)(O)$_2$]$^{2+}$ with H$_2$Q in CH$_3$CN can be represented by Eqs. (60) and (61):

$$trans\text{-}[Ru^{VI}(L^2)(O)_2]^{2+} + H_2Q$$

$$\xrightarrow[\text{CH}_3\text{CN}]{k_{ACN}} trans\text{-}[Ru^{IV}(L^2)(O)(CH_3CN)]^{2+} + Q + H_2O \quad (60)$$

$$trans\text{-}[Ru^{IV}(L^2)(O)(CH_3CN)]^{2+} + H_2Q$$

$$\xrightarrow[\text{CH}_3\text{CN}]{k'_{ACN}} trans\text{-}[Ru^{II}(L^2)(CH_3CN_2)]^{2+} + Q + H_2O \quad (61)$$

Rate constants at 298.0 K for the first (k_{ACN}) and second step (k'_{ACN}) are $(8.53 \pm 0.32) \times 10^1$ and (2.21 ± 0.04) M^{-1} s^{-1}, respectively. $\Delta H^{\ddagger}$ and $\Delta S^{\ddagger}$ are (12.3 ± 0.3) kcal mol^{-1} and $-(9 \pm 1)$ cal mol^{-1} K^{-1}, respectively, for the k_{ACN} path, (12.4 ± 0.3) kcal mol^{-1} and $-(15 \pm 2)$ cal mol^{-1} K^{-1}, respectively, for the k'_{ACN} path.

Rate constants for the oxidation of various substituted hydroquinones by Ru^{VI} in H$_2$O and in CH$_3$CN are summarized in Table 3.

Plots of log(k_{H_2O}, k_{ACN} or k'_{ACN}) at 298.0 K against the O–H BDE of H$_2$Q-X are linear for reactions in both H$_2$O and CH$_3$CN (Fig. 11), consisting with a HAT mechanism for these substrates. In these plots the O–H BDEs calculated according to the method of Wright et al. are used [36], since experimental data for only a few substrates such as H$_2$Q and H$_2$Q-Me are available. Notably H$_2$Q-2,5-di-^{t}Bu reacts more slowly than expected from its BDE, by about 50%. The presence of two bulky groups in the 2- and 5-positions should reduce the chance of hydrogen atom abstraction by the bulky *trans*-[Ru^{VI}(L^2)(O)$_2$]$^{2+}$ complex by about 50%.

Such steric effects are expected for a HAT mechanism but not for simple electron transfer.

Mayer and co-workers have recently shown that the Marcus cross-relation (neglecting work terms) holds fairly well for a range of PCET/HAT reactions [2b,23b–e].
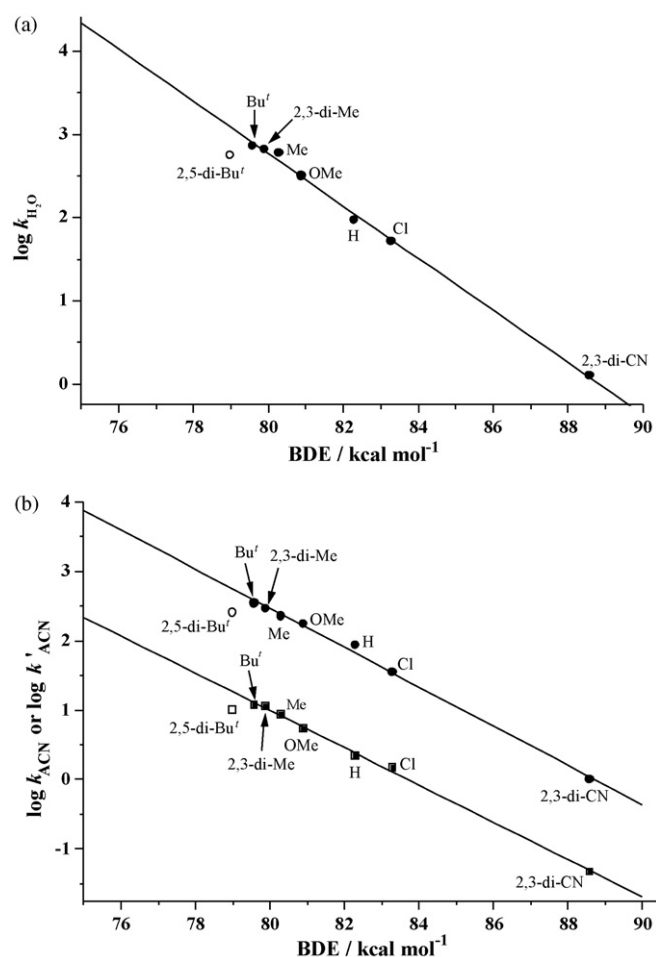
Fig. 11. (a) Plot of log k_{H_2O} vs. O–H BDE for the oxidation of H$_2$Q-X by *trans*-[Ru^{VI}(L^2)(O)$_2$]$^{2+}$ in aqueous solution at 298.0 K, pH 1.77 and $I = 0.1$ M. (b) Plot of log k_{ACN} (circles) and log k'_{ACN} (squares) vs. O–H BDE for the oxidation of H$_2$Q-X by *trans*-[Ru^{VI}(L^2)(O)$_2$]$^{2+}$ and *trans*-[Ru^{IV}(L^2)(O)(CH$_3$CN)]$^{2+}$, respectively, at 298.0 K in CH$_3$CN [32].

Table 4
Mechanistic summary for *trans*-$[Ru^{VI}(L)(O)_2]^{2+}$ systems[a]

Reductants	Pathway	Rate law	Rate constants	Remarks
$[Fe(H_2O)_6]^{2+}$[b]	e-Transfer	$-\dfrac{d[Ru^{VI}]}{dt} = k_2[Ru^{VI}][Fe^{2+}]$	$k_2 = 27.4\ M^{-1}\ s^{-1}$[c]	An inner-sphere mechanism is proposed
$[Ru^{II}(NH_3)_4(bpy)]^{2+}$[b]	e-Transfer	$-\dfrac{d[Ru^{II}]}{dt} = k_2[Ru^{VI}][Ru^{II}]$	$k_2 = 2.4 \times 10^6\ M^{-1}s^{-1}$[d]	The self-exchange rate of the *trans*-$[Ru^{VI}(L^2)(O)_2]^{+/2+}$ couple is estimated to be $1.5 \times 10^5\ M^{-1}\ s^{-1}$
$H_2PO_2^{-}$[e], $H_2PO_3^{-}$[e]	Hydride abstraction	$-\dfrac{d[Ru^{VI}]}{dt} = \dfrac{k}{1 + [H^+]/K_a}[Ru^{VI}][P]$	For hypophosphite, $k = 1.3\ M^{-1}\ s^{-1}$[c]. For phosphite, $k_2 = 4.8 \times 10^{-2}\ M^{-1}\ s^{-1}$[c]	For hypophosphite, $k(H_2PO_2^{-})/k(D_2PO_2^{-}) = 4.1$. For phosphite, $k(HDPO_3^{-})/(D_2PO_3^{-}) = 4.0$
Akylaromatic compounds[e]	Hydrogen atom abstraction	$-\dfrac{d[Ru^{VI}]}{dt} = k_2[Ru^{VI}][ArCH_3]$	For toluene $k_2 = 3.70 \times 10^{-5}\ M^{-1}\ s^{-1}$. For DHA $k_2 = 7.45\ M^{-1}\ s^{-1}$	(1) Plot of $\Delta H^{\ddagger}$ vs. $\Delta S^{\ddagger}$ is linear. (2) A linear correlation between $\Delta G^{\ddagger}$ and ΔH° is found. The slope of (0.61 ± 0.06) is in reasonable agreement with the theoretical lope of 0.5 predicted by Marcus theory
Phenol[e]	Hydrogen atom abstraction	$-\dfrac{d[Ru^{VI}]}{dt} = \left(k_x + \dfrac{k_y K_a}{[H^+]}\right)[Ru^{VI}][PhOH]$	$k_x = 12.5\ M^{-1}\ s^{-1}$[d], $k_y = 7.96 \times 10^8\ M^{-1}\ s^{-1}$[d]	(1) Linear correlation between $\log k_x$ vs. BDE of phenols is observed. (2) The rates constants are subjected to steric effects by bulky groups in the *ortho* positions
Hydroquinone[d]	Hydrogen atom abstraction	$-\dfrac{d[Ru^{VI}]}{dt} = \dfrac{k_a[H^+] + k_b K_a}{[H^+] + K_a}[Ru^{VI}][H_2Q]$	$k_a = 9.41 \times 10^1\ M^{-1}\ s^{-1}$[d], $k_b = 7.91 \times 10^7\ M^{-1}\ s^{-1}$[d]	(1) At pH 1.79, $k(H_2O)/k(D_2O) = 4.9$, At pH 4.60, $k(H_2O)/k(D_2O) = 1.20$. At both pH, $k(C_6H_4(OH)_2)/k(C_6D_4(OH)_2) = 1.0$. (2) In aqueous solution, the final product is *trans*-$[Ru^{IV}(L^2)(O)(OH_2)]^{2+}$ while in CH_3CN, the final product is *trans*-$[Ru^{II}(L^2)(CH_3CN)_2]^{2+}$. (3) Plots of log (rate constant) against the O–H BDE of H_2Q-X are linear. (4) Plots of $\log k_{12}$ vs. $\log K_{12}$ are linear and the slopes obtained are in reasonable agreement with the theoretical slope predicted by the Marcus equation. (5) The $[Ru^{VI}(L^2)(O)_2]^{2+}/[Ru^{V}(L^2)(O)(OH)]^{2+}$ self-exchange rate in CH_3CN is estimated to be $4 \times 10^2\ M^{-1}\ s^{-1}$
NO_2^{-}[e]	Reversible oxygen atom transfer	$-\dfrac{d[Ru^{VI}]}{dt} = \dfrac{k}{1 + [H^+]/K_a}[Ru^{VI}][NO_2^{-}]$	$k = 2.33 \times 10^4\ M^{-1}\ s^{-1}$[d]	(1) *trans*-$[Ru^{IV}(L^1)(O)(ONO_2)]^{2+}$ is first formed which then undergoes slow aquation. (2) ^{18}O-scrambling occurs in products
SO_3^{2-}[b]	Oxygen atom transfer	$-\dfrac{d[Ru^{VI}]}{dt} = \dfrac{k}{1 + [H^+]/K_a}[Ru^{VI}][S^{IV}]$	$k = 7.0 \times 10^4\ M^{-1}\ s^{-1}$[c]	The formation of a sulfato ruthenium(IV) intermediate is proposed
I^{-}[b]	Oxygen atom transfer	$-\dfrac{d[Ru^{VI}]}{dt} = (k_a + k_b[H^+])[Ru^{VI}][I^{-}]$	$k_a = 4.1 \times 10^{-2}\ M^{-1}\ s^{-1}$[d], $k_b = 18.5\ M^{-2}\ s^{-2}$[d]	Oxygen atom transfer from dioxoruthenium(VI) to I^{-} is proposed

[a] All the rate constants are at 298.0 K unless specified.
[b] Oxidant = *trans*-$[Ru^{VI}(L^2)(O)_2]^{2+}$.
[c] $I = 1.0\ M$.
[d] $I = 0.1\ M$.
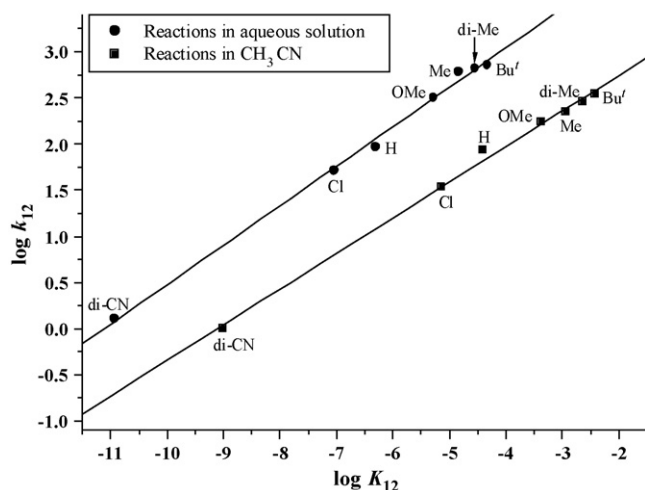[e] Oxidant = *trans*-$[Ru^{VI}(L^1)(O)_2]^{2+}$.

Fig. 12. Plot of $\log k_{12}$ vs. $\log K_{12}$ for the oxidation of H_2Q-X by *trans*-$[Ru^{VI}(L^2)(O)_2]^{2+}$ at 298.0 K in aqueous solution (circles) and in CH_3CN (squares) [32].

For reactions where the frequency factors, f_{12}, are close to 1, the Marcus cross-relation can be represented by Eq. (62).

$$k_{12} = (k_{11}k_{22}K_{12})^{1/2} \qquad (62)$$

k_{12} is the rate constant for the reaction between reactants 1 and 2. k_{11} and k_{22} are the H-atom self-exchange rates of the reactants. The equilibrium constant, K_{12}, for the oxidation of H_2Q-X by Ru^{VI} is calculated from $\Delta G^\circ = -RT \ln k_{12}$, using $\Delta G^\circ = \Delta H^\circ = $ O–H BDE of H_2Q-X $-$ BDE of $[O=Ru^V(L^2)O-H]^{2+}$. It is assumed that ΔS° for these reactions are relatively small. The BDE of $[O=Ru^V(L^2)O-H]^{2+}$ is calculated to be 73.7 kcal mol^{-1} in aqueous solutions and 76.3 kcal mol^{-1} in CH_3CN according to the equation: $D[O=Ru^V(L^2)O-H] = 23.06E^\circ + 1.37pK_a + C$ [23,24,30,37–39,40a]. E° for $[Ru^{VI}(L^2)(O)_2]^{2+}/[Ru^V(L^2)(O)_2]^+ = 0.56$ V (versus NHE) [4], pK_a of $[O=Ru^V(L^2)O-H]^{2+} = 2.8$ [4], $C = 57$ and 59.5 kcal mol^{-1}, respectively, in aqueous solutions and in CH_3CN [23d,30]. Fig. 12 shows plots of $\log k_{12}$ versus $\log K_{12}$ for the reduction of Ru^{VI} to Ru^{IV} by H_2Q-X in H_2O and in CH_3CN. Good linear correlations are obtained, the slopes of (0.43 ± 0.01) and (0.39 ± 0.01) for H_2O and CH_3CN, respectively, are reasonably close to the theoretical slope of 0.5 predicted by Eq. (62). Such linear plots imply that the H-atom self-exchange rates of the hydroquinones are similar. From the y-intercepts, which are equal to $(1/2)\log(k_{11}k_{12})$ according to Eq. (62), $k_{11}k_{22} = 1.1 \times 10^8$ and 1.1×10^7 M^{-2} s^{-2} for H_2O and CH_3CN, respectively. If the H-atom self-exchange rates of the hydroquinones in CH_3CN are taken as 3×10 M^{-1} s^{-1} [25], then the $[Ru^{VI}(L^2)(O)_2]^{2+}/[Ru^V(L^2)(O)(OH)]^{2+}$ self-exchange rate in CH_3CN is estimated to be 4×10^2 M^{-1} s^{-1}.

5. Summary and conclusions

Mechanistic summaries for the *trans*-$[Ru^{VI}(L)(O)_2]^{2+}$ systems are tabulated in Table 4.

In conclusion, *trans*-dioxoruthenium(VI) complexes containing macrocyclic tertiary amine ligands (*trans*-$[Ru^{VI}(L)(O)_2]^{2+}$)

are versatile oxidants that can react via a variety of pathways including outer-sphere one-electron transfer, inner-sphere one-electron transfer, hydrogen atom abstraction, hydride abstraction and oxygen atom transfer; the choice of pathway depends on the nature of the reductant.

These complexes are good one-electron oxidants because they have relatively high redox potentials (E° for $[Ru^{VI}(L)(O)_2]^{2+}/[Ru^V(L)(O)_2]^+$ are 0.94 V and 0.56 V for $L = L^1$ and L^2, respectively) and fast self-exchange rates (k for $[Ru^{VI}(L)(O)_2]^{2+}/[Ru^V(L)(O)_2]^+ \approx 1 \times 10^5$ M^{-1} s^{-1} at 298 K for $L = L^1$ or L^2). The Marcus cross-relation is useful to distinguish between inner-sphere and outer-sphere mechanisms.

These ruthenium oxo complexes are also good hydrogen atom abstraction reagents, as evidenced by a relatively large O–H bond dissociation energy for $[O=Ru^V(L)O-H]^{2+}$ (82.8 and 76.3 kcal mol^{-1} in CH_3CN for $L = L^1$ and L^2, respectively). They also have a reasonable hydrogen atom self-exchange rate (k for $[Ru^{VI}(L^1)(O)_2]^{2+}/[Ru^V(L^1)(O)(OH)]^{2+}$ in CH_3CN is around 2×10^1 M^{-1} s^{-1} at 298 K). Hydrogen atom abstraction by these complexes typically occur with large deuterium isotope effects $\{k(X–H)/k(X–D) = 5–15\}$. Log(rate constants) also show linear correlations with X–H bond dissociation energies.

These ruthenium oxo complexes are also good two-electron hydride abstraction and oxygen atom transfer reagents, as evidenced by their relatively high two-electron redox potentials (E° for $[Ru^{VI}(L)(O)_2]^{2+}/[Ru^{IV}(L)(O)(OH_2)]^{2+}$ are 1.22 V and 0.96 V at pH 1.0 for $L = L^1$ and L^2, respectively). The relatively slow oxygen exchange between these complexes and water is particularly useful for demonstrating oxygen atom transfer processes using ^{18}O labeling.

References

[1] (a) T.J. Meyer, M.H.V. Huynh, Inorg. Chem. 42 (2003) 8140;
(b) E.L. Lebeau, R.A. Binstead, T.J. Meyer, J. Am. Chem. Soc. 123 (2001) 10535;
(c) R.A. Binstead, M.E. McGuire, A. Dovletoglou, W.K. Seok, L.E. Roecker, T.J. Meyer, J. Am. Chem. Soc. 114 (1992) 173;
(d) R.A. Binstead, L.K. Stultz, T.J. Meyer, Inorg. Chem. 34 (1995) 546;
(e) S.A. Trammell, J.C. Wimbish, F. Odobel, L.A. Gallagher, P.M. Narula, T.J. Meyer, J. Am. Chem. Soc. 120 (2001) 13248;
(f) R.A. Binstead, T.J. Meyer, J. Am. Chem. Soc. 109 (1987) 3287;
(g) J. Gilbert, L. Roecker, T.J. Meyer, Inorg. Chem. 26 (1987) 1126;
(h) J.A. Gilbert, S.W. Gersten, T.J. Meyer, J. Am. Chem. Soc. 104 (1982) 6872;
(i) W.K. Seok, T.J. Meyer, Inorg. Chem. 44 (2005) 3931;
(j) M.S. Thompson, T.J. Meyer, J. Am. Chem. Soc. 104 (1982) 5070;
(k) L.E. Roecker, T.J. Meyer, J. Am. Chem. Soc. 108 (1986) 4066;
(l) L.E. Roecker, T.J. Meyer, J. Am. Chem. Soc. 109 (1987) 746;
(m) M.S. Thompson, T.J. Meyer, J. Am. Chem. Soc. 104 (1982) 4106;
(n) W.K. Seok, T.J. Meyer, J. Am. Chem. Soc. 110 (1988) 7358;
(o) L. Roecker, J.C. Dobson, W.J. Vining, Inorg. Chem. 26 (1987) 779;
(p) B.A. Moyer, K. Sipe, T.J. Meyer, Inorg. Chem. 20 (1981) 1475;
(q) W.K. Seok, J.C. Dobson, T.J. Meyer, Inorg. Chem. 27 (1988) 3;

(r) L.K. Stultz, R.A. Binstead, M.S. Reynolds, T.J. Meyer, J. Am. Chem. Soc. 117 (1995) 2520;
(s) L.K. Stultz, M.H.V. Huynh, R.A. Binstead, M. Curry, T.J. Meyer, J. Am. Chem. Soc. 122 (2000) 5984;
(t) W.K. Seok, T.J. Meyer, Inorg. Chem. 43 (2004) 5205.

[2] (a) T. Matsuo, J.M. Mayer, Inorg. Chem. 44 (2005) 2150;
(b) J.R. Bryant, J.M. Mayer, J. Am. Chem. Soc. 125 (2003) 10351.

[3] (a) C.M. Che, W.T. Tang, W.T. Wong, T.F. Lai, J. Am. Chem. Soc. 111 (1989) 9048;
(b) C.M. Che, T.F. Lai, K.Y. Wong, Inorg. Chem. 22 (1987) 2289;
(c) C.M. Che, W.T. Tang, W.O. Lee, W.T. Wong, T.F. Lai, J. Chem. Soc. Dalton Trans. (1989) 2011;
(d) C.M. Che, W.T. Tang, C.K. Li, J. Am. Chem. Soc. Dalton Trans. (1990) 3735.

[4] C.M. Che, K. Lau, T.C. Lau, C.K. Poon, J. Am. Chem. Soc. 112 (1990) 5176.

[5] C.M. Che, V.W.W. Yam, in: A.G. Sykes (Ed.), Advances in Inorganic Chemistry, vol. 39, Academic Press Inc., San Diego, 1992, p. 233.

[6] C.M. Che, V.W.W. Yam, in: C.M. Che, V.W.W. Yam (Eds.), Advances in Transition Metal Coordination Chemistry, vol. 1, Jai Press Inc., Greenwich, 1996, p. 209.

[7] C.M. Che, T.C. Lau, in: J.A. McCleverty, T.J. Meyer (Eds.), Comprehensive Coordination Chemistry II, vol. 5, Elsevier Pergamon, Amsterdam, 2004.

[8] R.A. Marcus, H. Eyring, Annu. Rev. Phys. Chem. 15 (1964) 155.

[9] T.C. Lau, K.W.C. Lau, C.K. Lo, Inorg. Chim. Acta 209 (1993) 89.

[10] J. Silverman, R.W. Dodson, J. Phys. Chem. 56 (1952) 846.

[11] P. Bernhard, A.M. Sargeson, Inorg. Chem. 26 (1987) 4122.

[12] J.T. Hupp, M.J. Weaver, Inorg. Chem. 22 (1983) 2557.

[13] R.B. Jordan, Reaction Mechanisms of Inorganic and Organometallic Systems, Oxford University Press, New York, 1991, Chapter 6.

[14] T.C. Lau, K.H. Chow, K.W.C. Lau, W.Y.K. Tsang, J. Chem. Soc. Dalton Trans. (1997) 313.

[15] (a) R. Sarala, M.A. Islam, S.B. Rabin, D.M. Stanbury, Inorg. Chem. 29 (1990) 1133;
(b) R. Sarala, D.M. Stanbury, Inorg. Chem. 29 (1990) 3456;
(c) L.I. Simándi, M. Jáky, C.R. Savage, Z.A. Schelly, J. Am. Chem. Soc. 107 (1985) 4220;
(d) J.M. Anast, D.W. Margerum, Inorg. Chem. 20 (1981) 2319;
(e) T. Ernst, M. Cyfert, M. Wilgocki, Int. J. Chem. Kinet. 24 (1992) 903;
(f) E.S. Gould, Acc. Chem. Res. 19 (1986) 66;
(g) G.P. Haight Jr., E. Perchonock, F. Emmenegger, G. Gordon, J. Am. Chem. Soc. 87 (1965) 3835.

[16] R.M. Smith, A.E. Martell, Critical Stability Constants, vol. 6, Plenum, New York, 1989.

[17] T.C. Lau, K.W.C. Lau, K. Lau, J. Chem. Soc. Dalton Trans. (1994) 3091.

[18] G. Nord, Comments Inorg. Chem. 13 (1992) 221.

[19] D.T.Y. Yiu, K.H. Chow, T.C. Lau, J. Chem. Soc. Dalton Trans. (2000) 17.

[20] W.L. Man, W.W.Y. Lam, W.Y. Wong, T.C. Lau, J. Am. Chem. Soc. 128 (2006) 14669.

[21] W.W.Y. Lam, S.M. Yiu, D.T.Y. Yiu, T.C. Lau, W.P. Yip, C.M. Che, Inorg. Chem. 42 (2003) 8011.

[22] C.M. Che, W.T. Tang, W.O. Lee, K.Y. Wong, T.C. Lau, J. Chem. Soc. Dalton Trans. (1992) 1551.

[23] (a) K.A. Gardner, J.M. Mayer, Science 269 (1995) 1849;
(b) K.A. Gardner, L.L. Kuehnert, J.M. Mayer, Inorg. Chem. 36 (1997) 2069;
(c) J.M. Mayer, Acc. Chem. Res. 31 (1998) 441;
(d) J.P. Roth, J.M. Mayer, Inorg. Chem. 38 (1999) 2760;
(e) J.P. Roth, S. Lovell, J.M. Mayer, J. Am. Chem. Soc. 122 (2000) 5486;
(f) G.K. Cook, J.M. Mayer, J. Am. Chem. Soc. 117 (1995) 7139.

[24] D.T.Y. Yiu, M.F.W. Lee, W.W.Y. Lam, T.C. Lau, Inorg. Chem. 42 (2003) 1225.

[25] J.P. Roth, J.C. Yodar, T.-J. Won, J.M. Mayer, Science 294 (2001) 2524.

[26] (a) J.K. Kochi (Ed.), Free Radicals, vol. 1, Wiley, New York, 1973;
(b) S. Korcek, J.H.B. Chenier, J.A. Howard, K.U. Ingold, Can. J. Chem. 50 (1972) 2285;
(c) J.M. Tedder, Angew. Chem. Int. Ed. Engl. 21 (1982) 401.

[27] P. Mulder, W. Saastad, D. Griller, J. Am. Chem. Soc. 110 (1988) 4090.

[28] M. Lucarini, P. Pedrielli, G.F. Pedulli, J. Org. Chem. 61 (1996) 9259.

[29] P. Franchi, M. Lucarini, G.F. Pedulli, L. Valgimigli, B. Lunelli, J. Am. Chem. Soc. 121 (1999) 507.

[30] J.M. Mayer, in: B Meunier (Ed.), Biomimetic Oxidations Catalyzed by Transition Metal Complex, Imperial College Press, London, 2000, p. 1.

[31] (a) P.K. Das, M.V. Encinas, S. Steenken, J.C. Sciano, J. Am. Chem. Soc. 103 (1981) 4162;
(b) A.J. Colussi, in: Z.B. Alfassi (Ed.), Chemical Kinetics of Small Organic Radicals, CRC Press, Boca Raton, 1988, p. 33;
(c) A. Baignee, J.A. Howard, J.C. Sciano, L.C. Stewart, J. Am. Chem. Soc. 105 (1983) 6120;
(d) D.V. Avila, K.U. Ingold, J. Lusztyk, J. Am. Chem. Soc. 117 (1995) 2929.

[32] W.W.Y. Lam, M.F.W. Lee, T.C. Lau, Inorg. Chem. 45 (2006) 315.

[33] A. McAuley, C.J. McDonald, L. Spencer, P.R. West, J. Chem. Soc. Dalton Trans. (1988) 2279.

[34] G.E. Adams, B.D. Michael, Trans. Faraday Soc. 63 (1967) 1171.

[35] C.M. Che, K.Y. Wong, C.K. Poon, Inorg. Chem. 25 (1986) 1809.

[36] J.S. Wright, E.R. Johnson, G.A. DiLabio, J. Am. Chem. Soc. 123 (2001) 1173.

[37] J.M. Mayer, I.J. Rhile, Biochim. Biophys. Acta 1655 (2004) 51.

[38] D.D.M. Wayner, E. Lusztyk, D. Page, K.U. Ingold, P. Mulder, L.J.J. Laarhoven, H.S. Aldrich, J. Am. Chem. Soc. 117 (1995) 8737.

[39] V.D. Parker, M. Tilset, J. Am. Chem. Soc. 111 (1989) 6711.

[40] (a) V.D. Parker, J. Am. Chem. Soc. 114 (1992) 7458;
(b) F.G. Bordwell, J.P. Cheng, G.Z. Ji, A.V. Satish, X. Zhang, J. Am. Chem. Soc. 113 (1991) 9790;
(c) D.R. Lide (Ed.), CRC Handbook of Chemistry and Physics, 82nd ed., CRC Press, Boca Raton, 2001.

[41] J.O. Howell, J.M. Goncalves, C. Amatore, L. Klasinc, R.M. Wightman, J.K. Kochi, J. Am. Chem. Soc. 106 (1984) 3968.